

2022-2023

Master Agronomie, Environnement, Territoires,
Paysage, Forêt (AETPF)

Major
Forests and their Environment

Assessing coupled process-based models' performance in predicting
tree mortality under climate change

Haoming ZHONG
Master thesis, defended at Nancy in 04/09/2023

Supervisor: Christian Piedallu, Research Engineer, AgroParisTech
Academic referent: Julien Sainte-Marie, Research Engineer, AgroParisTech

AKNOWLEDGEMENTS

This internship was conducted at EcoSilva, AgroParisTech, Nancy, in collaboration with the Center for Ecology and Evolutionary Ecology (CEFE), Montpellier, and the National Research Institute for Agriculture, Food and Environment (INRAE), Avignon, with the financial support from the FOREVERS project and Labex Arbre.

First and foremost, I would like to thank my supervisor Christian Piedallu, who accepted me for this internship and gave the most support during these months. I am very grateful for this research training that I have been taught thinking critically and processing data precisely and gained good habits for doing research. Christian's concern about climate change and the consequences on forests will always motivate me to do good and pragmatic research in the future. I appreciate all the effort he made for this internship.

I would like to thank Tanguy Postic and Xavier Morin for hosting me at CEFE. A special and great thanks to Tanguy, for the data preparation and detailed explanation whenever I asked question. I also would like to thank Nicolas Martin for the SurEau-Ecos and coupled link introduction, and his consistent guidance for determining research steps. I would also like to express my thanks to François de Coligny for the insightful Capsis platform training, Hélène Carletti for introducing me the mortality datasets, and Arsène Druel for assisting in soil parameter analysis. Finally, I would like to thank my academic referent Julien Sainte-Marie as well, who regularly tracked my progress and gave me suggestions when I met problems.

Due to the nature of remote online collaboration, it took more time and patience to facilitate effective communication and comprehension of the tasks at hand. I wish to express my gratitude once more to everyone involved for their dedicated efforts.

I would like to give a sincere hug to my families and friends for their understanding and support as always.

Summary:

A global drought-induced mortality increase has been noticed with the rapid climate change. Several attempts have been made to understand and predict mortality, and now the focus is on using process-based model to simulate water transport through soil, plant and atmosphere, and result in the percent loss of conductivity, which determines plant hydraulic failure occurs. This study is the first time to couple a plant hydraulic model (SurEau-Ecos) with an individual based forest gap model (ForCEEPS) and a phenological species distribution model (PHENOFIT) together to predict drought-induced mortality. We used two validation datasets varying from spatio-temporal scale to test model's performance on plot/tree mortality prediction, and its sensitivity to soil water holding capacity (SWHC). We compared the key parameter Leaf area index (LAI) generated by model with two external datasets: Probav and Sentinel 2. We concluded that this coupled model has a limited predictive ability with potential to improve by using good quality of soil water input, validating through informative mortality dataset, and reaching equilibrium state before drought period simulation.

Keywords: coupling, process-based model, tree mortality, drought, leaf area index, soil water holding capacity.

List of abbreviation:

PLC: Percent loss of conductivity/percentage of cavitation

DBH: Diameter at breast height

NFI: National forest inventory

PET: Evapotranspiration

ONF: Office National des Forêts

PRELEV5: Indicateur de coupe (2e visites) extracted from NFI database, which is indicating the presence of a partial or total cut of the trees between 2 visits.

NINCID: Nature de l'incident extracted from NFI database, which is characterizing the nature of a possible incident occurring on the inventory point during past 5 years. =2 means mortality.

LAI: Leaf area index

SWHC: Soil water holding capacity

ESDAC: European soil data center

HR-VPP: High resolution vegetation phenology and productivity

Content

1. Introduction.....	7
1.1 Species ecology and mortality impact	7
1.2 What is mortality and its causes?.....	8
1.3 How can we predict mortality?.....	8
1.4 Plant hydraulic model: SurEau-Ecos.....	11
1.5 Objective of this study.....	12
2. Method.....	12
2.1 Model introduction.....	12
2.1.1 Description and comparison	12
2.1.2 Coupling steps	15
2.2 Validation datasets	17
2.2.1 Vosges dataset.....	18
2.2.2 NFI dataset	18
2.3 Model assessment	19
2.3.1 Mortality prediction	19
2.3.2 Comparison and sensitivity analysis.....	20
3. Results.....	21
3.1 Mortality prediction for Vosges dataset	21
3.2 Mortality prediction for NFI dataset.....	23
3.3 LAI and mortality.....	25
3.3.1 Sentinel 2 LAI and mortality.....	25
3.3.2 Comparison of ForCEEPS, Probav, and Sentinel 2 LAI	27
3.4 Sensitivity analysis of SWHC.....	27
4. Discussion.....	29
4.1 Limitation of validation dataset	29
4.2 LAI and SWHC.....	29
4.3 Reach equilibrium state.....	30
4.4 Future application.....	30

5. Conclusion.....	31
6. Reference.....	32
Appendix.....	38
1. <i>Schematic of ForCEEPS and PHENOFIT.....</i>	38
2. <i>Species included in NFI dataset.....</i>	38
3. <i>Ecological ingredients covered by Vosges dataset.....</i>	40
4. <i>An example of output files.....</i>	40
5. <i>Explanation of confusion matrix.....</i>	41
6. <i>Process of extracting LAI Sentinel 2 value.....</i>	41
7. <i>Confusion matrix for defining mortality.....</i>	42
8. <i>Confusion matrix for comparing soil input data.....</i>	42

1. Introduction

1.1 Species ecology and mortality impact

Silver fir (*Abies alba*) and Norway spruce (*Picea abies*) are two of the most important conifer species in Europe with high economic and ecological importance (Caudullo et al., 2016; Dobrowolska et al., 2017). Compared to the ecology of two species, both of them show a preference for moist and cool conditions with nourishing acid soils. However, spruce exhibits a higher root water demand in comparison to fir (Piedallu et al., 2016). Silver fir, has experienced several droughts in the last century but demonstrated remarkable resilience and plasticity recovering after disturbances (Cailleret et al., 2014; Dobrowolska et al., 2017; Senf et al., 2020). With the changing of climate, the resilience of silver fir to drought has significantly decreased (Vejpustková et al., 2023). Norway spruce, renowned for its rapid growth and straight trunk morphology, has been widely cultivated out of its natural range in Europe since the 18th century due to its high commercial interest (Caudullo et al., 2016). However, it has received clear warnings about its vulnerability to drought (Lévesque et al., 2013), and now is facing an alarming trajectory of significant decline and escalating mortality rates in recent years due to the adverse changes in climate conditions (Krejza et al., 2021; Thiele et al., 2017).

The causes of dieback are complex and multifactorial. The dieback event was triggered by periods of extreme weather conditions, such as droughts and heatwaves, which increased the stress on the weakened trees and made them more susceptible to further damage from pests and pathogens. Higher temperatures contribute to the expansion of bark beetle populations, which exacerbate the damages and trigger mortality for fir and spruce (Allen et al., 2010; Anderegg, 2015; Choat et al., 2018; McDowell et al., 2022). Given the ongoing climate change, it is predicted that both species, particularly the Norway spruce, will encounter increasingly challenging and stressful conditions, leading to a substantial rise in mortality rates (Arend et al., 2021).

Mortality is an important ecological process in forest ecosystems that can affect different ecosystem services (Anderegg et al., 2013). Large-scale dieback of trees such as spruces in lowlands and uplands of central Europe can cause irreversible damage to local ecosystems (Mensah et al., 2021). This will have significant impacts on provisioning services such as wood production, as well as regulating services such as flood control, water management, and carbon sequestration. It will also influence cultural services that are closely linked to human well-being (Banerjee et al., 2013). Furthermore, dieback affect forest management and forestry decisions, especially in Europe where the forestry industry is well developed. For example, Douglas fir, a popular fast-growing tree species, has been extensively introduced for planting in Europe, but its enthusiasm for planting has been locally slowed down due to severe damage by bark beetles (Via. Private sawmill owner). Therefore, understanding and limiting tree mortality is of great ecological and economic significance.

1.2 What is mortality and its causes?

The general concept of tree mortality refers to various forms of tree-related deaths, from the death of a part of the tree to large-scale disturbances (Harmon and Bell, 2020). It is usually divided into background mortality and mortality caused by extreme events, such as insect-induced mortality and drought-induced mortality (Taccoen et al., 2019). The understanding of forest mortality varies at different time and space scales (Harmon and Bell, 2020). For example, in the development of forest succession, tree mortality is a normal and necessary process, allowing the forest to evolve from a single pioneer species to a diversified mixed forest through natural selection and competition mechanisms (Rohner et al., 2012). In this study, we mainly focus on the mortality increase caused by rapid changes in natural environmental conditions due to human impact and the concept of tree mortality mainly focuses on the lifespan of tree species as the time scale and an individual tree or plot as the spatial scale.

With the continuous rise in global temperatures, an increase in tree mortality rates has been observed worldwide, from boreal forests, tropical forest to temperate forest (Brienen et al., 2015; Hammond et al., 2022; Hubau et al., 2020; Liu et al., 2023; Van Mantgem et al., 2009). The rising mortality is not limited to the background mortality but is particularly pronounced when associated with drought and heatwaves. Focusing on coniferous forests, this situation is more apparent (Arend et al., 2021; Bianchi et al., 2021; Lévesque et al., 2013; Piedallu et al., 2023). The causes of tree mortality are diverse. Traditional mechanistic framework of tree mortality originates from Manion representing as a death spiral (Manion, 1991), which categorized the factors causing tree mortality into predisposing factors, inciting factors, and contributing factors. Predisposing factors refer to conditions that make trees more susceptible to death, such as old age, genetic vulnerabilities, prior stressors. Inciting factors are immediate triggers that directly cause tree mortality, including windstorms and severe weather events like heatwaves and drought. Contributing factors can exacerbate existing stresses and are most of the time caused by biotic attacks.

1.3 How can we predict mortality?

To further investigate the mechanisms of interaction and mutual influence among these factors, researchers have made various attempts to understand and predict tree mortality. These attempts include observing the drought response by tree ring (Bigler and Bugmann, 2004; Cailleret et al., 2014; Suarez et al., 2004; Williamson et al., 2000), the application of empirical models to decipher mortality patterns (Hulsmann et al., 2018; Maringer et al., 2021), and the implementation of mechanistic models to simulate the underlying physiological and ecological mechanisms linked to tree mortality (Davi and Cailleret, 2017; Li et al., 2022; McDowell et al., 2008, 2011; Seidl et al., 2011).

Initial observations were facilitated by long-term forest permanent plots, revealing significant spikes in annual mortality rates following events like the 1997 El Niño drought in the Amazon and widespread evergreen tree mortality in Argentina's national park (Suarez et al., 2004; Williamson et al., 2000). However, with the changes of plot location, collection protocol, and potential bias brought from analysis, these limitations challenge their

representation of broader stand variability across regions of interest (Fridman and Stahl, 2001; Sheil, 1995). Building upon data from forest plots, researchers have employed statistical and empirical models to predict mortality. Techniques range from linear and logistic regression to neural networks (Hasenauer et al., 2001; Hulsmann et al., 2018; King, 1996; Peng et al., 2011; Thripleton et al., 2021), to study correlations with observed mortality. As research advances, the focus shifts toward process-based models that incorporate physiological insights (Anderegg et al., 2015, 2012; Li et al., 2022; Liu et al., 2021; Martínez-Vilalta et al., 2002; McDowell et al., 2008; Ruffault et al., 2022). Fig. 1 shows the current models range from empirical to process-based approaches regarding scales from local processes and dynamics to global vegetation and general ecosystem models (Ruiz-Benito et al., 2020). In general, process-based models are utilized to depict the behavior of forests, employing a set of interconnected processes across varying scales. These processes mutually influence each other and interface with the surrounding environment (Gonçalves et al., 2021). Types of process-based model include understanding and predicting species distribution (Elith et al., 2006; Guisan and Zimmermann, 2000), forest dynamics and functioning (Bugmann, 2001; Keane et al., 2001; Morin et al., 2021), or focusing on simulating specific environmental process, such as hydrological model (Christoffersen et al., 2016; Cochard et al., 2021; Martinez-Vilalta et al., 2019) and carbon cycling model (Huang et al., 2020).

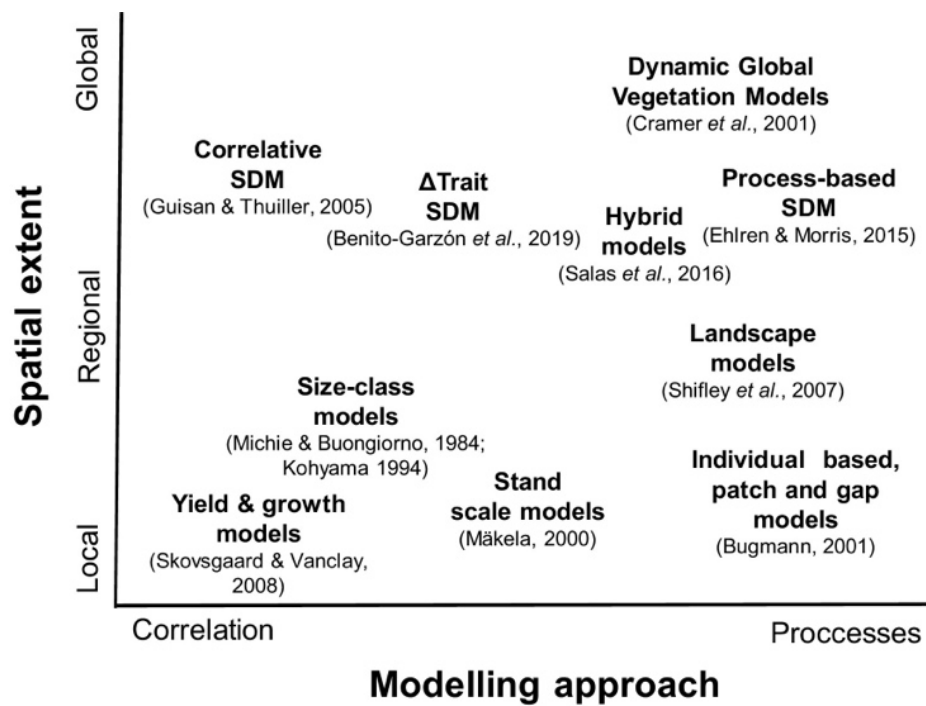


Figure 1. Existing modelling approaches. (Ruiz-Benito et al., 2020)

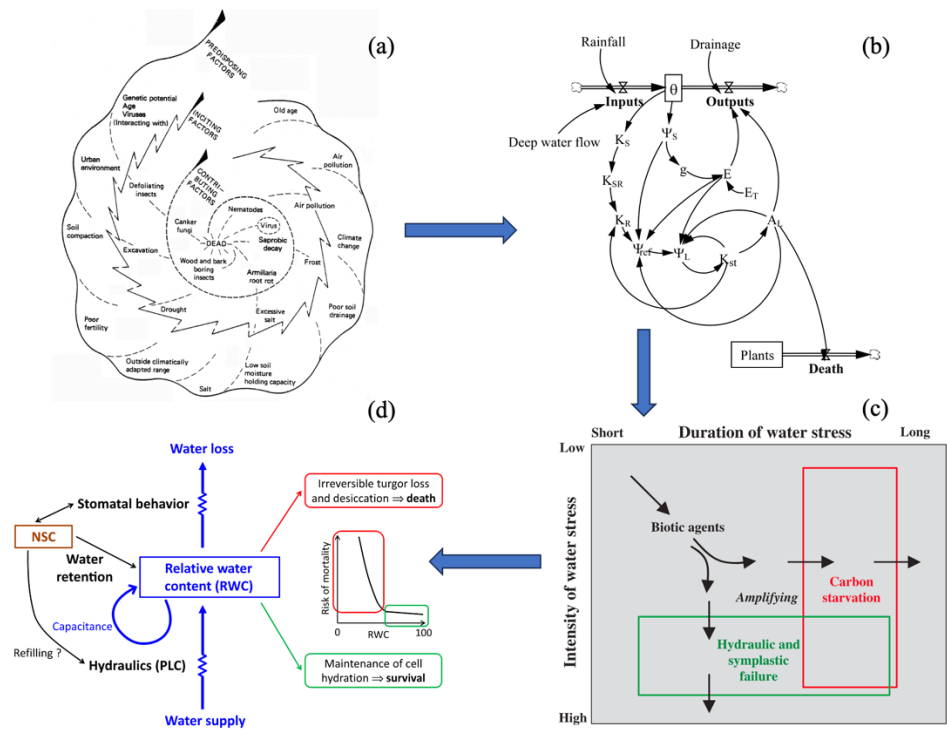


Figure 2. Progression of mechanistic framework for predicting mortality. (McDowell, 2021)

a. Mortality spiral framework; b. water transport in one plant; c. Theoretical relationship between drought characteristic and mortality pathways; d. plant relative water indicates mortality risk.

When we more focus on how to predict mortality using process-based model, there are several researchers (Manion, 1991; Martinez-Vilalta et al., 2019; Martínez-Vilalta et al., 2002; McDowell et al., 2008, 2011) tried to find the comprehensive functions and links that related to tree mortality based on Manion's mortality spiral framework (Fig 2, (a)). As shown in Fig. 2, framework (b) simulated water transport within individual woody plant; (c) discussed about the hydraulic failure or carbon starvation will contribute to death related to the intensity and duration of drought; and (d) presented a new link between mortality risk and plant relative water content considering hydraulics, carbon economy and stomal responses. We can conclude from cutting-edge research that plant hydraulic failure and carbon starvation are the two primary pathways triggered by drought and potentially lead to mortality (Brodrribb, 2020). During a drought, the initial impact is a decline in root water uptake, leading to reduced available water pools. As evaporation persists from plant surfaces, these water pools rapidly deplete. Consequently, sapwood embolism occurs, which, if it worsens beyond the recovery point, ultimately results in plant death—this is known as hydraulic failure (McDowell et al., 2022). On the other hand, in the early stages of drought, plants can mitigate functional damage by closing their stomata to limit water loss. However, this compromises carbon uptake and hampers plant growth. Prolonged stomatal closure increases the risk of death due to carbon starvation caused by insufficient food supply (McDowell et al., 2008). Plant hydraulic failure is typically modeled as the progressive loss of hydraulic conductivity, expressed as a percentage of conductivity loss across the entire plant or different organs (Martinez-Vilalta et al., 2019). Carbon starvation is modeled as the depletion of available non-structural carbohydrates (Liu et al., 2021). However, linking both processes in a model remains challenging, and the underlying interdependencies between

water and carbon within plants leading to system-level failure during mortality are still not fully understood by the scientific community (Martinez-Vilalta et al., 2019; McDowell et al., 2008; Sala et al., 2010). And there is still a doubt for taking the amount of non-structural carbohydrates as the indicator for carbon starvation (McDowell, 2021). Therefore, it is essential to initially focus on key processes first that capture the coarse and major mortality necessary for simulating forest response and mortality under climate change (Anderegg et al., 2012). Modeling the movement of water within plants from soil to the atmosphere, while considering the interplay among roots, stems, and leaves to simulate plant hydraulic failure, holds significance due to the pivotal role of water stress in driving tree mortality.

1.4 Plant hydraulic model: SurEau-Ecos

SurEau, a plant hydraulic model, employs a network of resistances and capacitances to simulate the soil-plant-atmosphere system and calculates water exchanges until stomatal closure occurs. It possesses the capability to describe the temporal variation of a plant's water status, encompassing water potential and water content, even beyond the point of stomatal closure (Cochard et al., 2021). It can translate meteorological data such as precipitation and evaporative demands into plant water content and xylem tension, which is crucial for simulating drought-induced mortality using process-based models (Blackman et al., 2016). The inclusion of explicit details and changes in each plant organs allows for accurate predictions of mortality for individual plants. However, the drawback of small timestep (seconds to minutes) approach is associated with high computational cost. To address this limitation and enable large-scale predictions, SurEau-Ecos was developed with a reduced number of parameters and computational cost. Despite this simplification, both models exhibit similar plant organ conductances and water reservoirs. However, a minor discrepancy is observed, with SurEau-Ecos underestimating the time to leaf hydraulic failure by 3 days (out of 90 days) compared to SurEau (Ruffault et al., 2022). Nonetheless, SurEau-Ecos provides the potential for predicting hydraulic failure and ecosystem vulnerability on a regional scale.

Integrating a mechanistic process into process-based models provides equal or improved predictive power over traditional process-model. (McDowell et al., 2013). Therefore, in this study, we tried to couple three different models together and estimated its ability for mortality prediction on different scales. The main model is ForCEEPS, which simulates tree establishment, growth, and survival within discrete patches, facilitating short-term forest growth predictions and long-term community composition forecasts (Morin et al., 2021). Notably, its strength lies in accounting for intra-species differences, wherein identical trees of the same age and under equivalent climatic conditions exhibit varying growth rates due to specific light competition factors (Postic, 2022). First it was integrated with a phenology process-based model PHENOFIT (Postic, 2022), functioning as a species distribution model and estimating the likelihood of a given species' presence across multiple years under distinct environmental conditions (Chuine and Beaubien, 2001). This coupling step has regulated establishment submodel and improved growth submodel in ForCEEPS (Postic, 2022), enabling the coupled model to encompass abiotic influences filtering on seed production and establishment within shifting climate scenarios. After incorporating SurEau-Ecos as a new

mortality submodel will allow us to take into account the risk of embolism and better understand forest dynamics in the context of climate change by considering both local dynamics and large-scale changes (Postic, 2022).

1.5 Objective of this study

The models (Chuine and Beaubien, 2001; Morin et al., 2021; Ruffault et al., 2022) have been coupled and parameterized by the CFE Laboratory in the aim to simulate forest dynamics but their ability to predict tree mortality has not yet been studied (Postic, 2022). In this study, we employed two datasets with different spatial and temporal scales describing mortality events for different species in the Vosges mountains and for the whole France to gauge the coupled model's efficacy in predicting mortality. Additionally, we explored the impact of Leaf area index and Soil water holding capacity changes on the coupled model's performance.

The study's objectives encompass the following:

- (1) For Vosges dataset, assessing the model's capability to predict drought-induced mortality on plot scale and replicate spatial mortality patterns for Fir and Spruce species, and evaluate its capacity to differentiate mortality risk for these two species.
- (2) For NFI dataset, investigating the model's performance to predict drought-induced mortality on plot and tree scale for a large number of species at the national extent.
- (3) Analyzing different LAI value and the relationship between LAI and mortality, and the sensitivity of SWHC within the coupled model that could have potential to influence the final predictive outcomes.

2. Method

This joint study engaged three institutes: CFE Montpellier, INRAE Avignon, and AgroParisTech Silva, with around 7 colleagues. CFE and INRAE led the model coupling work, while AgroParisTech conducted mortality assessment. The method mainly includes three parts: model introduction, validation datasets, and model assessment.

2.1 Model introduction

Here we will introduce the three different models and the coupling links among them. As this study is analyzing mortality prediction, we will more focus on the SurEau-Ecos model, which is the key model to predict mortality, and the link between SurEau-Ecos and ForCEEPS.

2.1.1 Description and comparison

ForCEEPS is the main body of this coupled model, which is an individual gap model based on the light competition simulating forest growth, dynamics, and evolution. After coupling with PHENOFIT, it is also able to simulate species distribution changes, based on the assumption that plant's survival and reproductive are driven by plant phenology. Finally coupling with SurEau-Ecos, will help to enhance the mortality submodule with specific hydraulic mechanisms and species hydraulic traits. The schematic representation of coupling link between ForCEEPS and PHENOFIT will be presented in Appendix 1.

The table 1 compare the three models from their purpose, approach, represented compartments and ecological processes, minimum spatial scale, and minimum time step. We can see all of them using process-based method but simulate forest regarding different compartments and processes, because they have very different purposes and applied scale. They consider mortality caused by light competition and hydraulic failure respectively.

Table 1. General information of three models (Marion, 2023 in review).

Model name	Purpose	Modelling approach	Compartment represented	Ecological process represented	Min spatial scale	Min time step
ForCEEPS	Simulate short-term forest growth and long-term forest composition	Process-based model (Gap model)	Stand Soil	Growth; PET; Rainfall interception; Runoff infiltration; Regeneration fitness; Mortality competition	Patch	Year
PHEONO TFIT	Predict species distribution based on phenology	Process-based model (Phenologic al model)	Stand Leaf Branch Flower and fruit Stem Bud Soil	Growth; PET; Photosynthesis; Respiration; Carbon allocation; Rainfall interception; Runoff infiltration; Drainage; Cavitation; Stomatal Conductance; Water potential plant/soil; Phenology; Regeneration fitness	Stand	Day
SurEau-Ecos	Simulate water flux and stock through plant's apoplast and symplast from soil to atmosphere	Process-based model (Plant hydraulic model)	Stand Leaf Branch Stem Root Organ Soil	Photosynthesis; Respiration; PET; Rainfall interception; Runoff infiltration; Cavitation; Stomatal conductance; Water potential plant/soil; Phenology; Regeneration fitness; Mortality hydraulic failure	Stand	Hour

SurEau-Ecos

The key model we considered for predicting drought-induced mortality is SurEau-Ecos (Ruffault et al., 2022), which simulates plant water status by considering water fluxes and stocks through the soil, plant, and atmosphere. It relies on a set of plant traits, soil properties, and meteorological data for its simulations. As shown in Fig. 3, in SurEau-Ecos, plant is treated as two organs: leaf and stem. The stem includes the woody volume of branches, trunk, and roots. Each of the two organs is described by its symplasmic (intracellular) and apoplasmic (extracellular) compartments. Soil is represented as a three-layer bucket whose physical properties allow the estimation of soil water retention and hydraulic properties. The model calculates water fluxes from the soil to the atmosphere through the leaf and stem as the product of an interface conductance and the difference between water potentials.

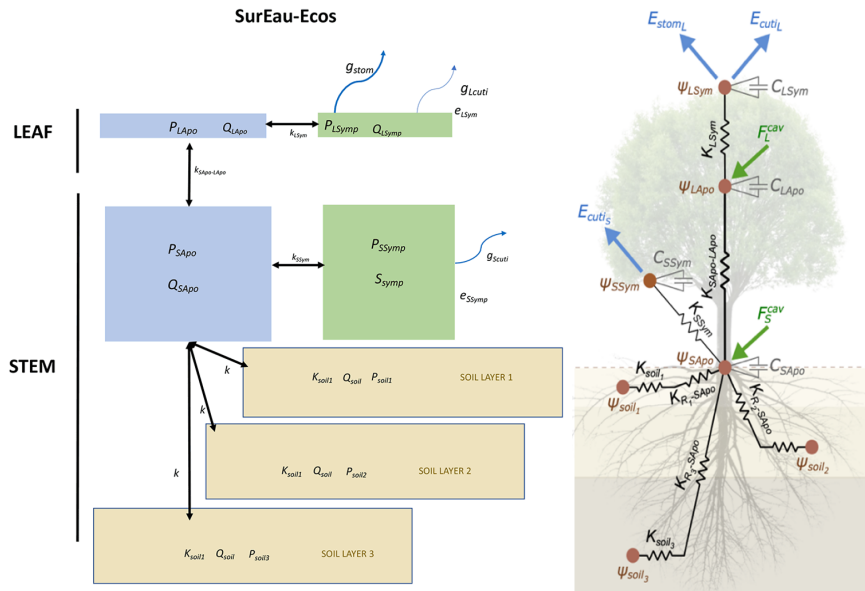


Figure 3. Plant architecture in SurEau-Ecos. (Ruffault et al., 2022)

Q indicates water quantities of the compartments, P is the water potential, K is the hydraulic conductance, g_s is the gaseous stomatal conductance, g_{cut} is the gaseous cuticular conductance. The subscripts “Apo” and “Sym” indicate apoplasm and symplasm compartments.

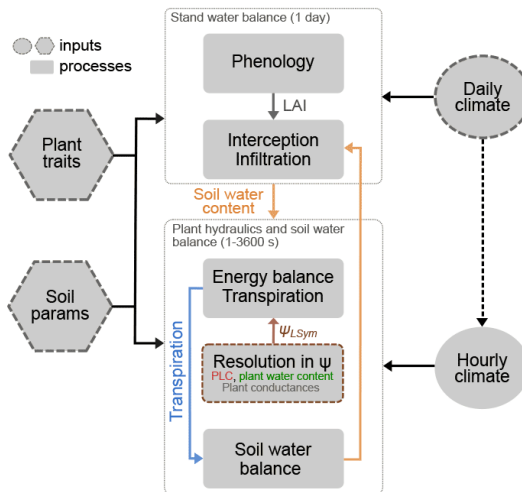


Figure 4. Simplified workflow in SurEau-Ecos. (Ruffault et al., 2022)

For the moment, the SurEau-Ecos can be executed using the R programming language or on CAPSIS platform. As seen in Fig. 4, the model needs plant hydraulic traits, soil parameters and daily climate data as inputs. During the running process, water dynamics (represented by nodes in Fig 1. right) of the soil-plant-atmosphere (SPA) system are locally governed by a generic partial differential equation (Eq. 1) for water mass conservation:

$$\frac{dq}{dt} = \nabla \cdot (k \nabla \psi) + s \quad (Eq. 1)$$

where q is the water quantity (kg/m^3), k is the conductivity, ψ is the water potential, $k\nabla\psi$ is the water fluxes, and s is the local sink term (i.e., a negative sign for soil evaporation or

transpiration) or source term (i.e., a positive sign for precipitation and water released by cavitation).

For each compartment (Fig. 3 left), water quantity, conductivity, potential, and fluxes are calculated. Water quantity is calculated as the rate of change of the water quantity per unit of leaf area (Q) using a volumetric integration method. Conductivity is calculated as the inverse of the hydraulic resistance of the soil-plant-atmosphere system. Water potential is calculated using the van Genuchten-Mualem model, which relates water potential to soil water content. Water fluxes between two adjacent compartments are simulated using Darcy's law as the product of compartment's interface conductance (K_{ij}) and the gradient of water potential (ψ). Water balance is calculated using different generic soil water balance equations for soil and plant compartments that considers water fluxes, soil properties, and meteorological data. More specific introduction of model principle can be found in Ruffault et al. 2022.

SurEau-Ecos provides several outputs including water dynamics, plant physiology, ecosystem functioning etc. Here we will focus on the outputs related to plant hydraulic, such as leaf PLC (percent loss of conductivity/percentage of cavitation), stem PLC, leaf water status, mean stomatal closure etc. Especially the PLC, could relate to the likelihood of tree mortality.

2.1.2 Coupling steps

Due to its complexity spanning multiple spatial and temporal scales, accurately modeling the forest while considering all ecological processes is challenging. Coupling models presents a potential solution. One important concern is to avoid overlaps, especially avoiding a plant being penalized twice for the same factor (Postic, 2022). We will use a specific example to explain the modelling coupling, assuming that we are going to simulate the forest dynamics on one patch (circle with 15m radius) for 11 years since 2008 (Fig. 5).

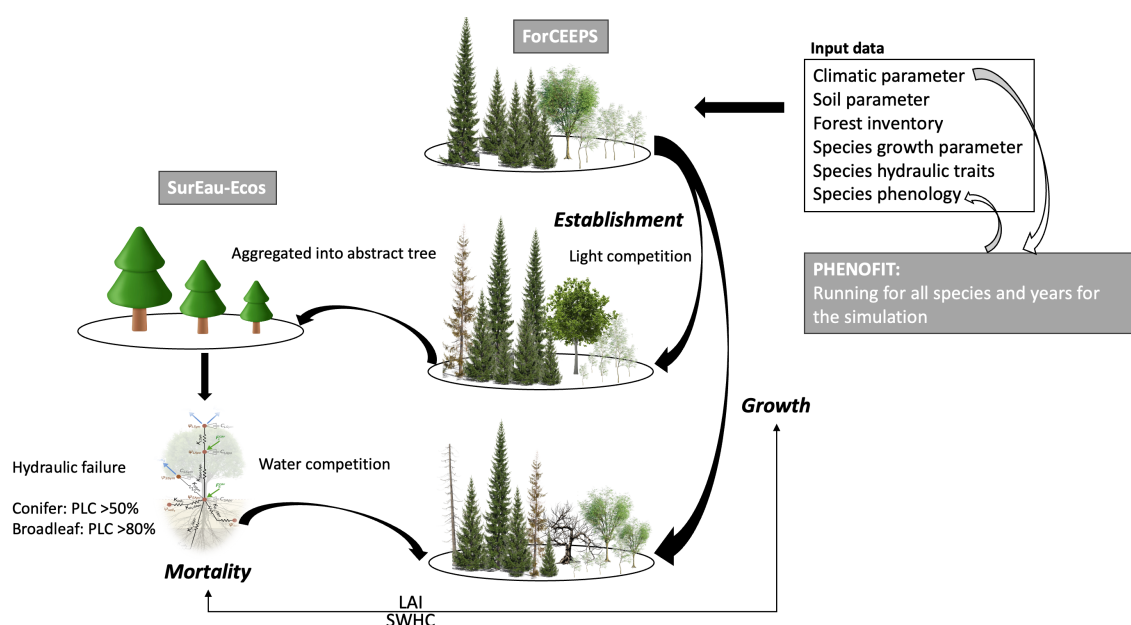


Figure 5. Illustration of coupling model. (Tree icons are free sources from Internet)

Firstly, based on climatic, soil data, and species phenology parameters, we started running PHENOFIT model from 2008 to 2019. The intermediate results of this model: each species' leaf phenology (leaf unfolding and leaf senescence dates), frost damage, and reproductive success data for each year on this patch, will be used as input data for ForCEEPS. By running PHENOFIT, we will make sure the species will distribute in their fundamental niche. Secondly, combining with forest inventory and species parameters data, ForCEEPS will start the simulation for each individual tree on this patch for each year. Trees establish, grow and die are the essential parts of forest dynamics. ForCEEPS establishment submodule is driven by bioclimatic parameters, browsing index, LAI generated by itself and reproductive success from first step. Here considers intraspecific and interspecific light competition and several physiological constrains, such as drought index, growing degree days, and animal browsing. For the growth submodule, the optimal growth of each tree was estimated based on species parameters: growth rate, specific allometric parameters and maximum reachable height and age, etc. Then the realized tree growth was determined from optimal growth combining with a series of growth reduction factors: drought, growing degree days (regulated by leaf unfolding and leaf senescence dates from first step), soil reduction, crown length, light availability, and frost damage reduction from first step. More specific introduction can be found in Appendix1. Last is ForCEEPS's mortality submodule which is completely replaced by SurEau-Ecos model for this study. For saving computational cost and time, all the tree on this patch will be aggregated to several representative trees grouped by species and classes of tree sizes. Leaf and stem biomass based on LAI generated from ForCEEPS was provided to SurEau-Ecos. Combining with plant hydraulic traits parameters, SurEau-Ecos will be executed, providing a PLC value (percent loss of conductivity/percentage of cavitation), which could be an indicator for plant hydraulic failure and will be sent back to ForCEEPS. Then the mortality for each tree will be determined randomly using a logarithmic probability distribution. Based on the literature review, we determine that for coniferous and broadleaves species, if the PLC is over 50% and 80% respectively, we consider it died because of plant hydraulic failure.

At the end, we will have two type of output file for each plot: complete file and mean file. The complete file includes the dendrometry information for each year about patch ID, speciesID, age, height, volume, crown length, DBH, LAI, basal area etc. The mean file includes the average value of each dendrometric index and site bioclimatic index for each year and each plot. One important remark is that this coupling work is still ongoing by Tanguy Postic (CEFE Montpellier), and several parts need to be improved. Therefore, our analysis is based on the semi-final coupled model and could provide feedback for future improvement. In table 2, we listed six types of input parameters with description and sources. The climate parameter is extracted and corrected from Digitalis and ERA-5 land dataset (Postic, 2022). Because former is a monthly dataset with a finer spatial resolution (1 km), while latter is a daily dataset with a coarser spatial resolution (8 km).

Table 2. Description and source of input parameters for coupled model.

Model inputs	Description	Sources
Climate parameter	Monthly and daily climatic data include temperature, precipitation, solar radiation, humidity, wind speed etc.	Climatic model Digitalis V2b (Silva lab) ERA-5 Land (Muñoz-Sabater et al., 2021)
Soil parameter	Including rock fraction, height, saturation capacity, vanGenuchten parameters for three soil layers.	Field mearsurment (Piedallu et al., 2013) ESDAC (Panagos et al., 2012)
Forest inventory	Including species composition, age, DBH, height, crown area, previous DBH increment etc.	National Forest Inventory
Species parameter	Max height and age, growth rate, min degree days for germination, min and max. winter temperature tolerance, leaf area, etc.	ForCEEPS (Morin et al., 2021)
Species hydraulic traits	Each species has around 50 plant physiological and ecophysiological parameters such as leaf mass, leaf vulnerability, and stomatal conductance, etc.	SurEau-Ecos (Cochard et al., 2021; Ruffault et al., 2022)
Species phenology	Including leaf survival index, leaf unfolding date, leaf senescence date, maturation index, and fruit survival index, etc.	PHENOFIT outputs

2.2 Validation datasets

Two datasets were used to validate the model's ability to predict tree mortality. First is a local dataset in Vosges and second is a French continental level NFI dataset. These two datasets are very different from each other regarding spatial scale, species included, and mortality collection method (Table 3).

Table 3. Comparison of the two datasets.

Dataset	Extent	Number of plots	Species with mortality information	Advantage	Disadvantage
Vosges	Vosges	1866	Norway spruce and Silver fir on 2019.	High plot density; sampling optimized to detect mortality patterns.	Ecological information extracted from GIS models, stand characteristics from aerial photographs, and mortality from remote sensing.
NFI	France	1694	65 common species in France from 2010 to 2020. (Appendix 2)	Tree and stand description obtained by field survey; a lot of species considered.	Low plot density; few observed mortality.

2.2.1 Vosges dataset

The Vosges, situated in northeastern France, cover an area of 8900 km², of which approximately 60% is densely forested (Benoit, 2022). Due to available datasets collected in previous studies (Piedallu et al., 2013), we narrow our focus to the prominent Norway spruce and Silver fir, which collectively dominate the Vosges mountain landscape, presenting in 53% and 59% of the species, respectively. The mortality dataset was extracted via Sentinel-2 imagery from 2019. The Sentinel-2 data's classification yielded an 92% accuracy in distinguishing between healthy and mortality plots with an independent validation dataset (Piedallu et al., 2023).

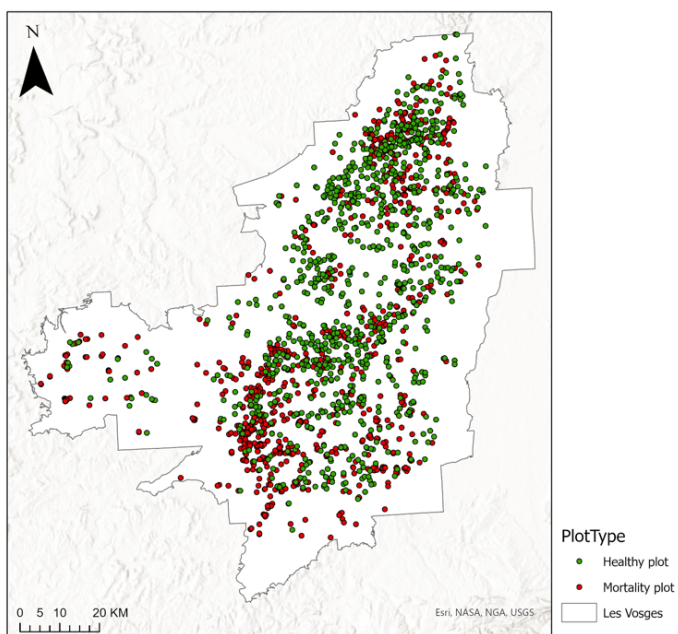


Figure 6. Distribution of Spruce and Fir in Vosges plots.

The Vosges dataset encompasses 1866 plots with the presence of mortality and some basic information describing the stand characteristics obtained by photointerpretation (Fig. 6). Within each plot, a comprehensive array of approximately 150 explanatory variables is incorporated, encompassing essential details such as stand characteristics, topographical insights, soil, and climatic factors. A noteworthy challenge encountered in harnessing this dataset for coupling models arises from the absence of authentic forest inventory data containing comprehensive stand characteristics. To surmount this issue, each plot was paired with a NFI forest inventory dataset, based on congruence in stand structure, density, species composition, and proximity to forest boundaries. We employed 764 NFI forest inventory records to simulate the dendrometry characteristics required by the models for the 1866 plots. Ecological ingredients covered by this dataset can be seen in Appendix 3.

2.2.2 NFI dataset

The second dataset originates from NFI France and was obtained through a rigorous filtering process. We examined sites that underwent twice repeated inventory assessments from 2010 to 2020, excluding those subjects to any cutting activities (PRELEV5 = 0) while focusing on instances of notable mortality (NINCID = 2). This process led to the identification of a total

of 702 sites demonstrating mortality occurrence. Concurrently, we selected a distinct set of controlled sites (a total of 992), ensuring their characteristics encompassed absence of both mortality and any cutting interventions. There are 65 common species in France considered in this NFI dataset (Appendix 2). As Fig. 7 shows the mortality plots are mainly located in mountainous areas.

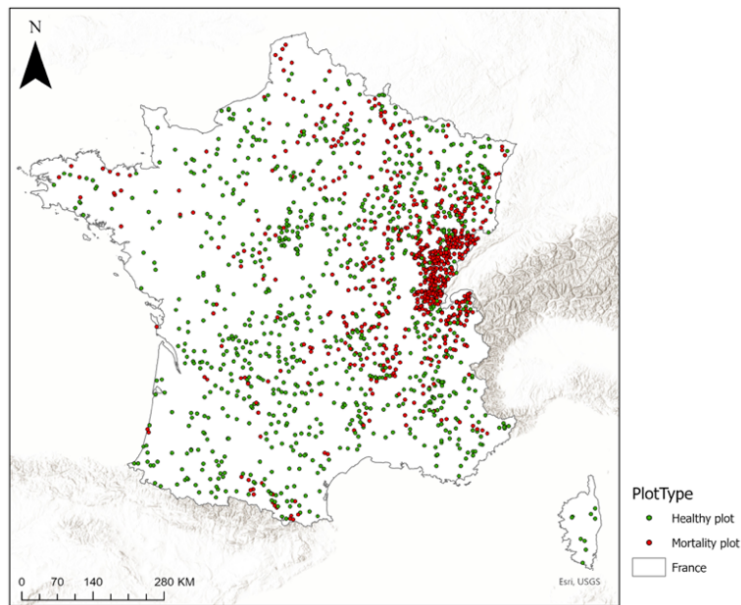


Figure 7. Distribution of NFI plots.

2.3 Model assessment

The model's assessment encompasses three parts: an analysis of mortality prediction, LAI comparison and SWHC sensitivity analysis.

2.3.1 Mortality prediction

For each plot, we utilized files that encompass dendrometry details for every tree, spanning from the start to the end of the simulation period. In the case of the Vosges dataset, the simulation spans from 2008 to 2019, while for the NFI dataset, it entails rolling five-year periods from 2010 to 2020. An example of output file is provided in the Appendix 4.

Prior to delving into the analysis of mortality prediction, a prerequisite is to establish the criteria that delineate the occurrence of mortality using the coupled models. We have chosen three specific indices to demarcate mortality (Table 4.) for the Vosges dataset: Number of dead trees, loss of Leaf area index (LAI), and loss of Basal area. For each species, the comparison between the values of 2018 and 2019 were linked to observed mortality for the Vosges dataset, which describes the distribution of mortality in July 2019. For NFI dataset, we only used Basal area loss during simulation period for each plot as the mortality index. If the calculated index value assumes a negative value, it predicts mortality happened within that plot; conversely, a positive value indicates a healthy plot.

Table 4. Explanation of index.

Index	Vosges dataset	NFI dataset
Number of dead trees	$Number_{x_1y_1} - Number_{x_1y_2}$	
LAI loss	$LAI_{x_2y_1} - LAI_{x_2y_2}$	
Basal area loss	$BA_{average\ x\ y_1} - BA_{average\ x\ y_2}$	

For Vosges dataset, x_1 : Spruce or Fir separately, x_2 : all the species on the plot, y_1 : 2019, y_2 : 2018; For NFI dataset, x : all the species on the plot, y_1 : 2015-2020, y_2 : 2010-2015.

For assessing the effectiveness of our model's mortality prediction, given the binary nature of the tree status (healthy/mortality), we used a confusion matrix and spatial mapping to evaluate both accuracy and spatial trends. In this context, we defined instances of mortality as the positive cases. The tabulated representation outlines various scenarios: a plot classified as mortality by the model and indeed representing mortality is a true positive; a plot classified as healthy by the model despite being a mortality case is a false negative, and so forth. Subsequently, we apply the success of the model (Appendix 5. Eq. 2, table 3), sensitivity (Appendix 5. Eq. 3), and specificity (Appendix 5. Eq. 4) indices to gauge the model's performance.

2.3.2 Comparison and sensitivity analysis

Throughout the process of integrating these models, it has become evident that the performance of this coupled model is notably influenced by two key parameters: Leaf area index (LAI) and Soil water holding capacity (SWHC). LAI is a quantitative measure assessing the amount of leaf area per unit of ground area which is crucial for assessing vegetation health and productivity (Campbell, 1986). SWHC is the maximum amount of water that a particular soil type can retain and hold against the force of gravity, while still allowing air to circulate within the soil pores. This impacts plant growth and water availability (Campbell, 1986). ForCEEPS inherently generates its own LAI values based on stand characteristics. Consequently, our approach involves a comparative analysis of the LAI values produced by ForCEEPS with those from two external sources: LAI Probav and LAI Sentinel 2. This comparison will allow us to establish a comprehensive understanding of the LAI dynamics within the integrated framework. Shifting our focus to SWHC, we have conducted simulations employing two distinct datasets to facilitate an insightful evaluation. The first dataset originates from direct field measurements (Piedallu et al., 2013), while the second dataset is a combination of maximum rooting depth coefficient from the European Soil Data Centre (ESDAC) and field measurements (Panagos et al., 2012). By contrasting the outcomes of these simulations, we aim to scrutinize how the model's predictions fluctuate based on the selection of SWHC data sources. This comparative analysis serves as a critical step toward comprehending the model's sensitivity and enhancing its predictive capabilities.

LAI dataset

LAI generated by ForCEEPS was extracted from mean output file for each plot. LAI Probav was extracted Arsène Druel from INRAE. LAI Sentinel 2 was extracted by me from HR-VPP dataset (HR-VPP user manual, 2022). Detailed process can be found in Appendix 6. We compared the trend of LAI Sentinel 2 for 4 years determining its relationship with mortality pattern. As we assumed that mortality plots will have a decreasing LAI value. Then we

compared these three sources of LAI to evaluate the difference and LAI generated by ForCEEPS.

SWHC dataset

We possess two sets of soil data. The initial dataset stems from NFI data measured in-situ (Piedallu et al., 2013). For the sake of convenience, we designate this as the "Original Soil Dataset". This dataset provides the soil water holding capacity for the uppermost 1-meter soil layer and then transformed to soil water content. However, plant roots can extend much deeper in reality. As a result, we have prepared a second dataset that estimates the soil water holding capacity for the top 5 meters of the soil profile. To accomplish this, we applied a coefficient derived from the maximum rooting depth provided by the European Soil Data Centre (ESDAC) to the Original Soil Dataset. This revised dataset is denoted as the "Modified Soil Dataset".

3. Results

In this section, we will present the results of four aspects (Table 5): the quality of mortality prediction for Vosges dataset and the NFI dataset, the comparison of Leaf area index (LAI) and its relationship with mortality, and the sensitivity analysis of Soil water holding capacity (SWHC).

Table 5. Structure of the result.

Objective	Vosges dataset	NFI dataset
Species considered	Norway spruce and silver fir	37 species (Appendix 2)
Mortality prediction	x	x
LAI analysis	x	
SWHC analysis	x	x

3.1 Mortality prediction for Vosges dataset

With the dataset, we conducted a comparative analysis of the performance of three indices: Number of dead trees, Leaf area index (LAI) loss, and Basal area (BA) loss, to better define mortality with the coupled models. Both BA loss and the number of dead trees exhibit a more favorable suitability than LAI loss (Table 6). This result can be easily explained. For Spruce and Fir, BA loss and the number of dead trees are calculated only for Spruce and fir on the plot scale. Conversely, LAI loss is determined at the plot level, encompassing all species within that plot.

The success rates reveal only marginal disparities among the three indices, with BA loss slightly outperforming the other two indices for Spruce. We have chosen to adopt BA loss as the designated index for mortality definition at the plot level in the subsequent phases of our analysis. Fig. 8 shows the relationship between predicted BA loss with observed plot status. Because this coupled model has been validated for tree growth and BA loss has better confidence (Postic, 2022). The performance of mortality prediction is moderately accurate with room for improvement. Regarding the sensitivity index for Spruce (0.46) and Fir (0.14),

we can conclude that this model has a better ability of predicting mortality for Spruce than Fir. Detailed confusion matrix can be found in Appendix 7.

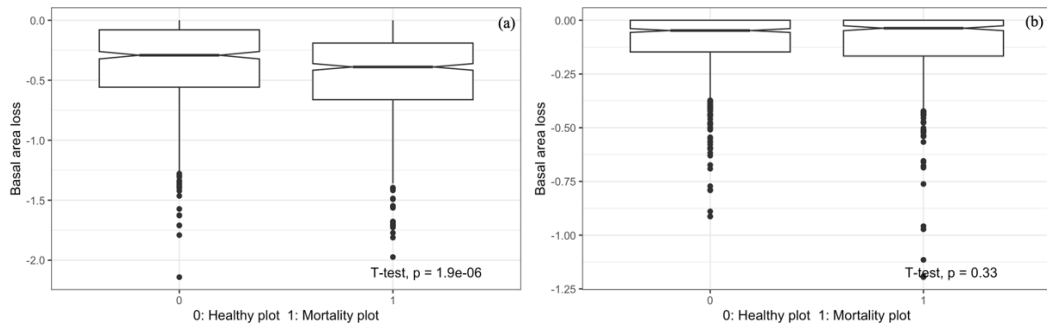


Figure 8. Predicted basal area loss against observed plot status for Spruce (a) and Fir (b).

Table 6. Performance of each index. (Sn: Sensitivity, Sp: Specificity)

Index	Spruce			Fir		
	Sn	Sp	Success	Sn	Sp	Success
Number of dead trees	0.43	0.59	0.50	0.14	0.86	0.55
LAI loss	0.34	0.67	0.48	0.30	0.70	0.53
BA loss	0.46	0.60	0.53	0.14	0.86	0.54

We compared the mortality frequency (Number of mortality plots / Number of plots) regarding two species (Table 7). First comparing the frequency between observation and prediction, we can see that observation has higher ratios than prediction, which means the mortality is underestimated for both species. Second comparing the frequency between Spruce and Fir of prediction, Fir has a much lower value than Spruce. Also comparing the ratio of predicted mortality plots to observed mortality plots, Spruce is much higher than Fir. This means coupled model has the potential to differentiate two species in predicting mortality.

Table 7. Mortality to healthy plots ratio comparison.

	Item	Spruce	Fir
Observation	Number of mortality plots	726	530
	Number of healthy plots	594	668
	Mortality frequency	0.55	0.44
Prediction	Number of mortality plots	570	167
	Number of healthy plots	750	1031
	Mortality frequency	0.43	0.14
Predicted number of mortality plots / Observed number of mortality plots		0.79	0.32

Figure 9 displays an even distribution of accurate predictions for both mortality and healthy plots across the study area. In the south-western region of the mountain range, there is a notable discrepancy between observed mortality and the predictions made by the coupled models, specifically regarding Fir (as indicated by the orange dots in Fig. 9). Here is a plateau with an average altitude of 600 to 800 meters and has experienced abundant rainfall in the past. However, recent years have witnessed significant drought events that have impacted

this region. The underlying reason for these inaccurate predictions may stem from the omission of species acclimation in this coupled model.

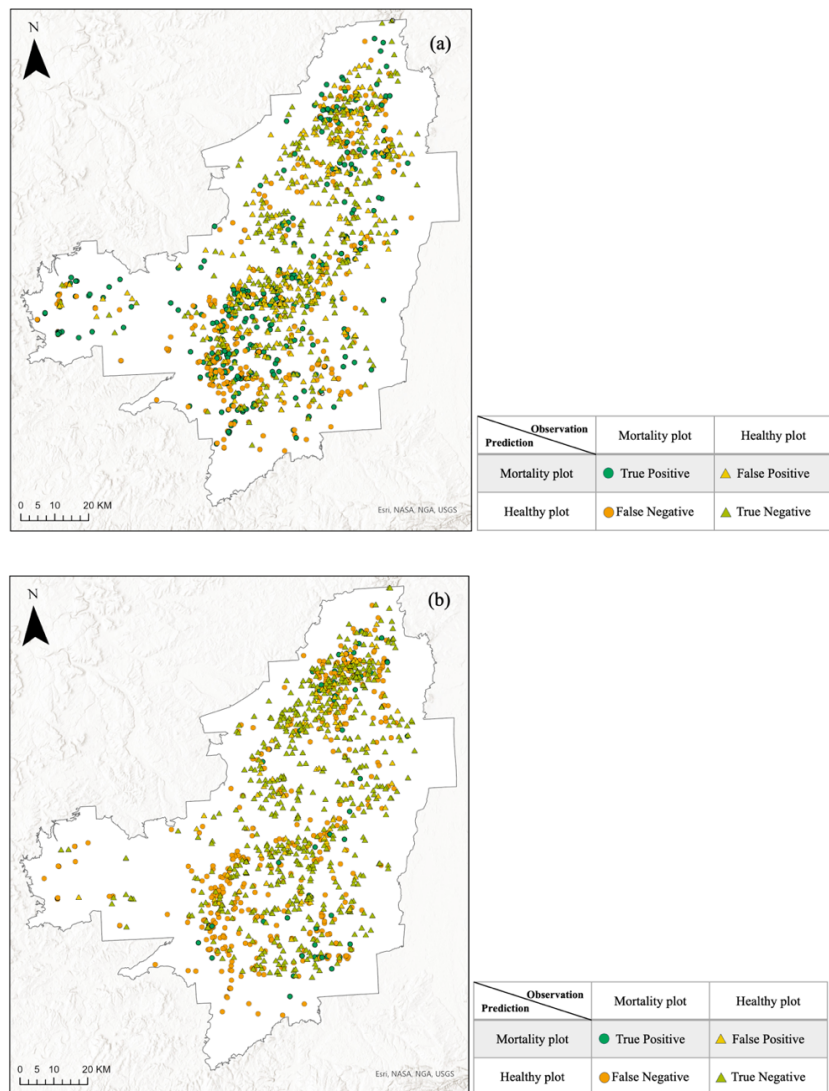


Figure 9. Quality of prediction distribution for Spruce (a) and Fir (b) in Vosges.

3.2 Mortality prediction for NFI dataset

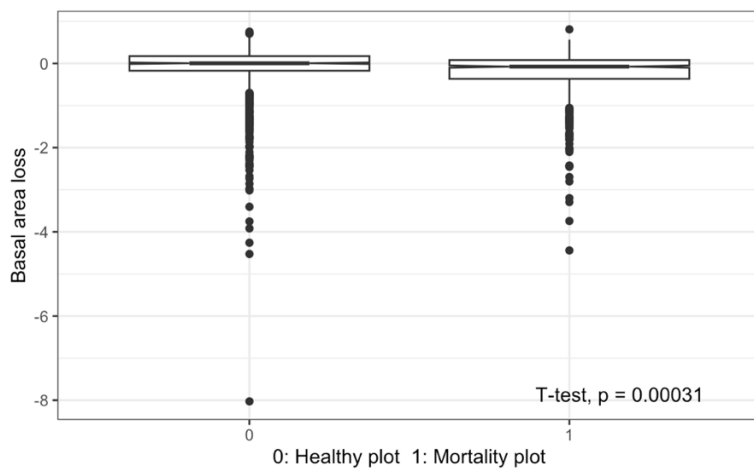


Figure 10. Predicted basal area loss against observed plot status for NFI dataset.

Fig. 10 shows that the predicted Basal area loss is not significantly different from healthy to mortality plots. The performance of the model for the NFI dataset is presented below for all the species combined, featuring the following metrics: Sensitivity (Sn) value: 0.61, Specificity (Sp) value: 0.55, and overall model success: 0.58. Comparing to Vosges dataset, NFI datasets has a slightly better prediction. The observed mortality-to-healthy plots ratio is 0.71, while the ratio for predicted mortality-to-healthy plots is 1.07 (Table 8). This indicates an overprediction of mortality for NFI dataset.

Table 8. Mortality to healthy plots ratio comparison.

	Item	NFI
Observation	Number of mortality plots	702
	Number of healthy plots	992
	Ratio	0.71
Prediction	Number of mortality plots	875
	Number of healthy plots	819
	Ratio	1.07

In Fig. 11, we visualized the distribution of mortality and healthy plots. We can see the accurate mortality predictions are concentrated in the Jura mountains. However, there are instances of incorrect predictions labeling them as healthy. In south of France, there's an overestimation of predicted mortality compared to observed.

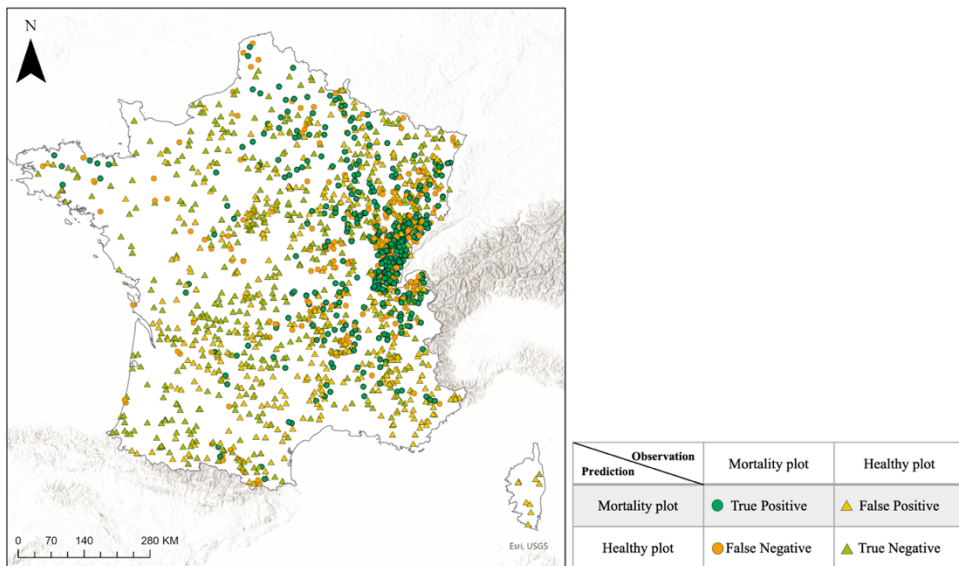


Figure 11. Prediction distribution for NFI dataset.

For the NFI dataset, we assessed mortality prediction for each species on tree scale. It's worth noting that the coupled model currently encompasses parameters for only 37 French common species, which means that the prediction for the NFI dataset was limited to these 37 species rather than the total 65 species observed in the forest. Fortunately, the species with high number of dead trees are included in the ForCEEPS simulation. For the species have not integrated, ForCEEPS also has represented standardized parameters for them. Detailed difference can be found in Appendix 2. It is important to emphasize again that this NFI dataset has been filtered by several factors and the result cannot represent the France national

forest. In table 9, we present the predicted number of dead trees, and in table 10, we provide mortality frequency for 9 selected species, comparing the predictions to observed values. Among these, the coupled model yielded relatively similar predicted numbers of dead trees for *Carpinus betulus* and *Castanea sativa*. However, for the remaining species, the model significantly underestimated the number of dead trees. In terms of mortality frequency, the model exhibited improved predictive capability, slightly overestimating it for 8 of the species but not for *Carpinus betulus*.

Table 9. Comparison of number of dead trees. (Highlighted the similar number)

Species	Observed Number of dead trees	Predicted Number of dead trees
<i>Fraxinus excelsior</i>	5416	881
<i>Picea abies</i>	2961	272
<i>Carpinus betulus</i>	2658	2494
<i>Castanea sativa</i>	2005	2032
<i>Corylus avellana</i>	1235	352
<i>Abies alba</i>	953	129
<i>Betula pendula</i>	671	314
<i>Populus tremula</i>	641	340
<i>Pinus sylvestris</i>	547	355

Table 10. Comparison of mortality frequency (%): Number of dead plots / Number of plots.

Species	Observed Frequency	Predicted Frequency
<i>Castanea sativa</i>	0.51	0.63
<i>Picea abies</i>	0.49	0.55
<i>Fraxinus excelsior</i>	0.49	0.51
<i>Corylus avellana</i>	0.37	0.28
<i>Pinus sylvestris</i>	0.34	0.55
<i>Populus tremula</i>	0.32	0.38
<i>Abies alba</i>	0.32	0.45
<i>Betula pendula</i>	0.27	0.37
<i>Carpinus betulus</i>	0.27	0.69

3.3 LAI and mortality

LAI is a crucial measure for understanding how forests grow and change over time. It is intriguing to find out if changes in LAI are connected to tree mortality. To investigate this, we examined four years of LAI data from Sentinel 2 to see if it relates to mortality caused by drought in 2018 in the Vosges. Additionally, it's important to check if the coupled model can generate LAI accurately. To do this, we compared the LAI data from ForCEEPS with data from Probav and Sentinel 2 for the Vosges dataset.

3.3.1 Sentinel 2 LAI and mortality

The median LAI value from Sentinel 2 ranges from 1.74 to 2.00, and exhibits a consistent trend over the years, with a decline in the mean LAI value, from 2.12 in 2017 to 1.81 in 2020 (Table 11). The standard deviation displays an upward trajectory over the course of these years.

Table 11. Statistical comparison of LAI for four years.

Index	2017	2018	2019	2020
Min	0.46	0.67	0.72	0.23
Max	6.41	6.30	6.69	5.92
Median	2.00	1.93	1.84	1.74
Mean	2.12	2.07	1.94	1.81
Std	0.59	0.59	0.64	0.66

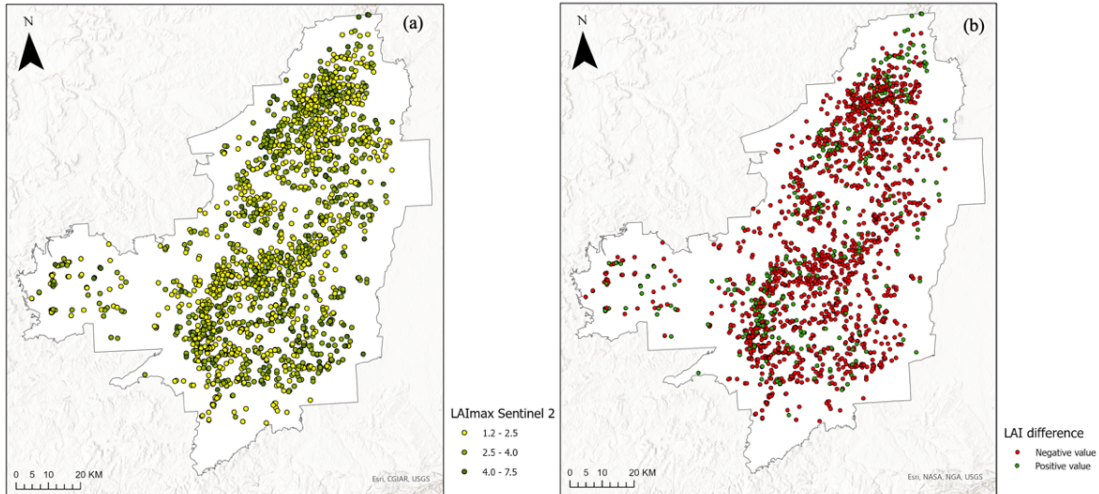


Figure 12. LAI max value from Sentinel 2 (a) and LAI difference (b).

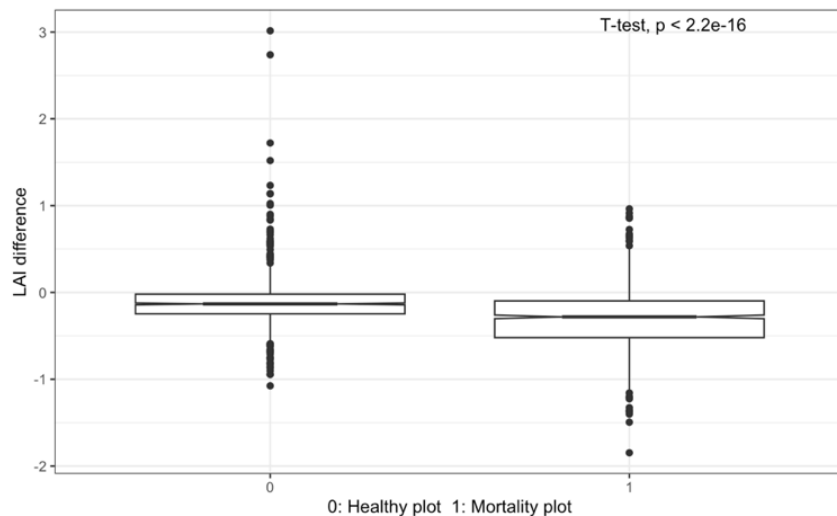


Figure 13. LAI sentinel 2 difference and plot status.

Fig. 12 (a) is the distribution of LAI max value and ranges from 1.24 to 7.53. Fig. 12 (b) is LAI difference calculated based on the average value of 2019 and 2020 minus average value of 2017 and 2018. From this map, we can see significant LAI decrease happened in the upper, left and bottom parts. And this pattern is consistent as the distribution of observed mortality (Fig. 6). We expect the LAI decrease can be due to the mortality increase (Fig. 13). The mean of LAI difference for healthy and mortality plots are significantly different from each other.

3.3.2 Comparison of ForCEEPS, Probav, and Sentinel 2 LAI

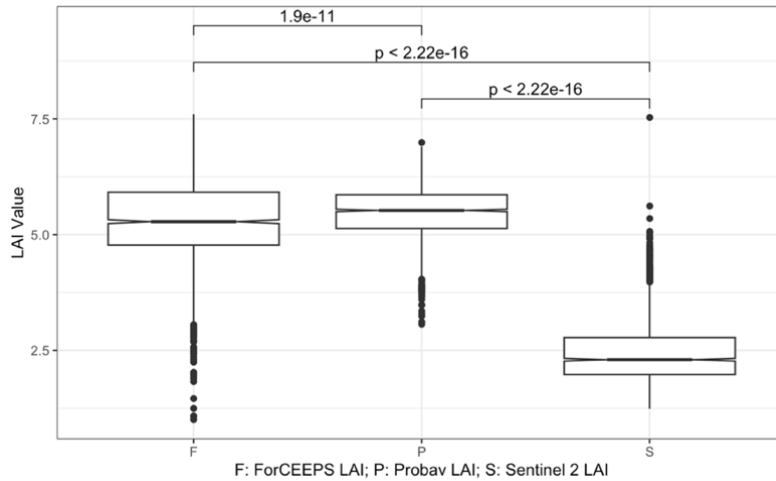


Figure 14. LAI values from ForCEEPS, Probav and Sentinel 2.

ForCEEPS LAI are LAIMax from 2017-2019; Probav LAI and Sentinel 2 LAI are LAIMax from 2017-2020.

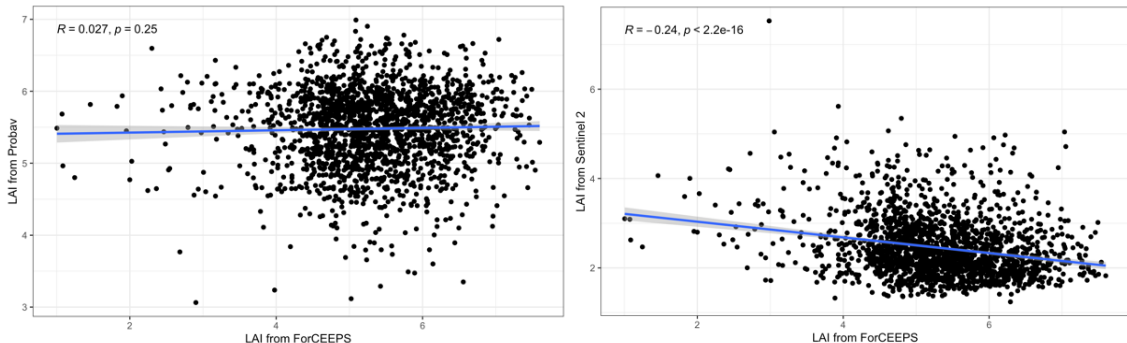


Figure 15. ForCEEPS LAI against Probav LAI (a) and Sentinel 2 LAI (b).

ForCEEPS LAI are LAIMax from 2017-2019; Probav LAI and Sentinel 2 LAI are LAIMax from 2017-2020.

From Fig. 14, we can see a similar value range for ForCEEPS LAI and Probav LAI. But Sentinel LAI has a much lower value compared to the others. One reason could be this dataset is not used for determining absolute but effective LAI value. From Fig. 15, we noted that ForCEEPS LAI has a week positive correlation with Probav LAI, which could be explained by the small scale of area. While the link between ForCEEPS LAI and Sentinel 2 LAI is very strange, and this could relate to the nature of Sentinel 2 LAI. We can conclude from this analysis is that three different LAI has small similarity and with a large uncertainty. This will be one of main limits when using this coupled model.

3.4 Sensitivity analysis of SWHC

Modified soil data values are logically higher than Original soil data (Fig. 16). And they have a weak positive correlation (Fig. 17). From ecological aspect, we expect better prediction for Modified soil data than Original soil data.

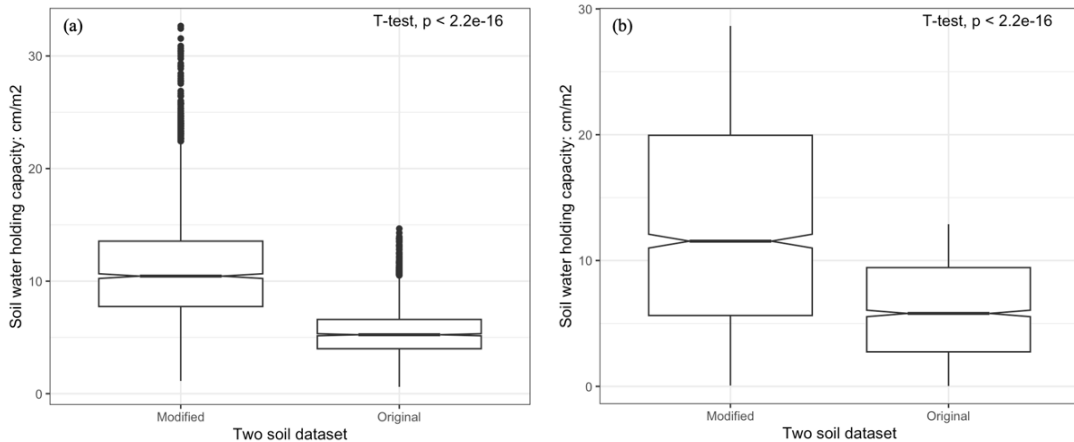


Figure 16. Soil water holding capacity comparison for Vosges (a) and NFI dataset (b).

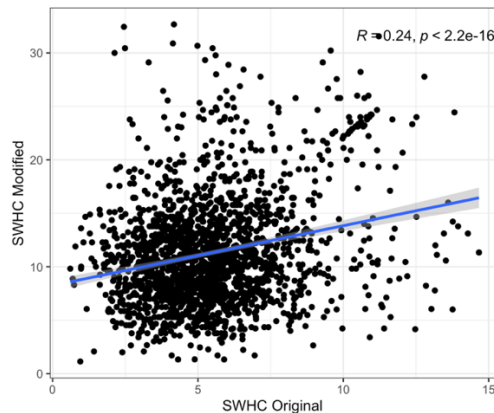


Figure 17. Soil water holding capacity comparison for Vosges dataset.

Table 12-13 present an overview of the model's performance for the Vosges and NFI dataset, considering two distinct sets of soil input data. Detailed confusion matrix can be found in Appendix 8. The "Modified soil input" exhibits superior model success and sensitivity compared to the "Original soil input" for both Vosges and NFI dataset. This improvement is particularly pronounced for Spruce, demonstrating a substantial enhancement in the model's ability to predict mortality when deeper soil prospection is considered. For NFI dataset, an elevated model success rate has been noted for the "Modified soil data", however, this comes with a trade-off of reduced sensitivity and increased specificity. We conclude that this coupled model is very sensitive to soil characteristics. The small changes in the calculation method have consequences on model's performances.

Table 12. Model performance for two different soil input for Vosges dataset. (Sn: Sensitivity, Sp: Specificity)

Soil input	Spruce			Fir		
	Sn	Sp	Success	Sn	Sp	Success
Modified soil data	0.46	0.60	0.53	0.14	0.86	0.54
Original soil data	0.11	0.90	0.43	0.10	0.88	0.51

Table 13. Model performance for two different soil input for NFI dataset. (Sn: Sensitivity, Sp: Specificity)

Soil input	Sn	Sp	Success
Modified soil data	0.61	0.55	0.58
Original soil data	0.85	0.27	0.51

4. Discussion

The predictive capability of our coupled model exhibits a certain degree of effectiveness, given slightly better performances comparatively to estimations of mortality estimated by chance (the model success ranges between 0.53 and 0.58 vs. 0.50 if it was estimated by chance). However, its performances remain weak, and our assessment has unveiled several limits stemming from validation dataset limitations, input parameter considerations, and equilibrium state.

4.1 Limitation of validation dataset

The nature of the validation datasets, particularly the Vosges dataset, can be a limit to this study. While mortality information is gathered through satellite image interpretation with a commendable 92% accuracy, the absence of comprehensive forest inventory data poses constraints. Vital inputs for the coupled model, such as species composition, canopy structure, and dendrometry, remain unavailable for each plot. To bridge this gap, forest inventory from the National Forest Inventory (NFI) database to the Vosges dataset were assigned based on corresponding stand characteristics. The slightly lower performance of the models comparatively to the NFI dataset could be attributed to this limit. However, this dataset allows an important number of plots with mortality recordings, at regional scale and at the species level, not available in the NFI dataset. For the NFI dataset, our approach involved selecting sites characterized by a lack of cutting activities over a 5-year period and a notable occurrence of mortality. As a result, the instances of mortality are concentrated within the mountainous areas. It may be attributed to the difficulties of accessing higher altitudes, where human harvesting might be less feasible. By consequence, a significant portion of mortality plots had to be excluded from the dataset. This exclusion was due to the sanitary cutting for dead trees that does not appear in the subsequent inventory.

Consequently, difficulties emerge in evaluating the model's ability due to the absence of high-quality mortality datasets. This has also been recognized by several other studies (Ruiz-Benito et al., 2020) that the mortality dataset is lack of temporal resolution and has no consistency on protocols (Hülsmann, 2021). To address this limitation, we have collected several complementary datasets. Moving forward, our strategy involves utilizing these new datasets for our next phase, offering the advantage of relatively comprehensive input parameters, enhancing our ability to further assess and refine the model's performance in predicting tree mortality dynamics.

4.2 LAI and SWHC

When considering the model's input parameters, two parameters emerge as particularly critical and sensitive: Leaf area index (LAI) and Soil water holding capacity (SWHC). The model autonomously generates LAI based on stand structure, necessitating the prerequisite of precise forest inventory data. Verification involves comparing the generated LAI with external data sources. This approach demonstrated important discrepancies at regional scale between the different sources estimated using remote sensing approaches. To better determine their performances, the use of field data would be necessary.

In the case of SWHC, we encounter challenges in acquiring precise data regarding root exploration depth. The task of capturing soil water content in this deeper layer is pivotal in simulating plant hydraulic failure. In this study, we employed field estimations of soil water content at a 1-meter depth to extrapolate to a 5-meter depth. The extrapolation to this latter depth exhibited enhanced predictive capabilities for mortality outcomes. This outcome underscores the indispensable role of a meticulously accurate soil input dataset in mortality prediction. A new soil dataset has been tested by Arsène Druel which is based on an ecohydrological assumption that forests adapt their overall available water capacity via root depth, to uphold a low embolism rate within standard conditions, considering a specific climate, traits blend, and Leaf area index (Druel et al., 2023; Eagleson, 1982). Although this work is in early stages, the preliminary results hold promise.

4.3 Reach equilibrium state

First, we need to discuss about the timestep we chose for this study. In the Vosges simulation, our temporal scope spans from 2008 to 2019. The reason is that a study by Benoit (2022) undertook a comparative assessment of climate evolution calculated between different periods of time on tree mortality, in the Vosges mountains. Climate evolution was calculated as the difference between historical climatic conditions (1961-1987) and various durations, spanning from 30 to 5 years before 2019. The study revealed a progressive elevation in temperature and evaporation deficit anomalies with shorter durations, with a stronger link with mortality patterns. In response, we opted for a 10-year timestep. For the NFI dataset, the simulation timestep entails rolling five-year periods from 2010 to 2020, contingent upon the date forest inventory observations. It will be useful to test if the simulation timestep has an influence on model's performance or not.

However, before we determine this, it is essential to note that achieving equilibrium within each plot before drought simulation is pivotal for enhancing result accuracy. In forest modeling, an "equilibrium state" signifies a balanced condition where ecological processes in the forest ecosystem stabilize over time (Stewart, 1986). Key processes like tree growth, mortality, reproduction, and nutrient cycling reach a consistent level under prevailing conditions. The forest's structure and functioning remain relatively stable, though variability persists, reflecting dynamic balance amidst biotic and abiotic factors. To accomplish this, we need to run the model utilizing climate data from a long historical period for each study plot. This will yield a resultant plot inventory that can serve as the initial forest inventory for simulating periods of drought. And it will also allow us to integrate the effect of acclimatization. Consequently, within the context of our coupled model, exploring different long-term simulation periods is relevant to assess the consistency of forest status with evolving timeframes.

4.4 Future application

When considering the forest's response to climate change, mortality emerges as one of the most uncertain processes (Bugmann et al., 2019). Over the years, researchers have attempted various methods to comprehend and forecast tree mortality across different forest types, yielding mixed outcomes (Anderegg et al., 2016; Meir et al., 2015; Trugman et al., 2021;

Venturas et al., 2021). Predicting tree mortality, from regional to global scales, has proven relatively challenging, with conflicting patterns even within the same region using different scales of process-based models (McDowell, 2021). Scientists acknowledge the difficulty of accurately predicting drought-induced tree mortality but see promise in using species hydraulic traits to simulate water transport, conductivity, and embolism (Anderegg et al., 2016; Choat et al., 2012). While addressing modeling methods, there remains the challenge of validation data (Ruiz-Benito et al., 2020). Current mortality datasets often consist of binary 0/1 entries with limited variation, while the exact causes of mortality are elusive in the field and absent from the data (Hülsmann, 2021). Associating mortality variations with their causes could undoubtedly enhance model performance. Fortunately, researchers advocate for and contribute to collecting mortality datasets globally, exemplified by the work of the International tree mortality network. Establishing a global protocol for data collection and compilation of worldwide mortality datasets is both necessary and pressing.

Under this global context, this study presents an attempt to employ a plant hydraulic model coupled with a forest gap model and a species distribution model to predict drought-induced mortality on regional and national scales for the first time. Despite encountering limitations, we have predicted 53%-58% of the distribution of the mortality (plot scale) from Vosges to the national scale of France. Our ongoing efforts involve addressing these limitations through more comprehensive datasets, integrating new soil water input data, refining model connections, and enhancing output formats. Subsequently, we plan to reevaluate its predictive capabilities. With improvements, we envision this coupled model evolving into a robust tool for assessing climate change's potential impacts on forest ecosystems, offering practical insights into forest management, and aiding decision-makers in the forestry sector.

5. Conclusion

This study is the first time to couple three different process-based model together to simulate forest dynamics and predict drought-induced mortality on regional and national scale. By addressing several existed limitations, the predictive ability will be improved in the near future, and it will help to answer theoretical questions regarding tree mortality: Where is the limit of drought tolerance for each species? Will trees grow slowly before drought occurs, and can we capture this pattern? Do larger trees bear a higher mortality risk than smaller ones, and can we quantify this phenomenon? Is the PLC threshold defining mortality for each species consistent across different forest types? It will also help to answer practical and concerned questions in forest sector: Which species are suitable to plant for regional area under different climate change scenarios? How can we recognize and facilitate assistant migration of endangered species? Does mixed forest cultivation enhance forest resilience and productivity? How to manage forest to optimize the balance among timber production, carbon storage, and water regulation? etc.

6. Reference

- Allen, C.D., Macalady, A.K., Chenchouni, H., Bachelet, D., McDowell, N., Vennetier, M., Kitzberger, T., Rigling, A., Breshears, D.D., Hogg, E.H., Gonzalez, P., Fensham, R., Zhang, Z., Castro, J., Demidova, N., Lim, J.-H., Allard, G., Running, S.W., Semerci, A., Cobb, N., 2010. A global overview of drought and heat-induced tree mortality reveals emerging climate change risks for forests. *For. Ecol. Manag.* 259, 660–684.
<https://doi.org/10.1016/j.foreco.2009.09.001>
- Anderegg, W.R.L., 2015. Spatial and temporal variation in plant hydraulic traits and their relevance for climate change impacts on vegetation. *New Phytol.* 205, 1008–1014. <https://doi.org/10.1111/nph.12907>
- Anderegg, W.R.L., Berry, J.A., Field, C.B., 2012. Linking definitions, mechanisms, and modeling of drought-induced tree death. *Trends Plant Sci.* 17, 693–700. <https://doi.org/10.1016/j.tplants.2012.09.006>
- Anderegg, W.R.L., Flint, A., Huang, C., Flint, L., Berry, J.A., Davis, F.W., Sperry, J.S., Field, C.B., 2015. Tree mortality predicted from drought-induced vascular damage. *Nat. Geosci.* 8, 367–371. <https://doi.org/10.1038/NGEO2400>
- Anderegg, W.R.L., Klein, T., Bartlett, M., Sack, L., Pellegrini, A.F.A., Choat, B., Jansen, S., 2016. Meta-analysis reveals that hydraulic traits explain cross-species patterns of drought-induced tree mortality across the globe. *Proc. Natl. Acad. Sci. U. S. A.* 113, 5024–5029. <https://doi.org/10.1073/pnas.1525678113>
- Anderegg, W.R.L., Plavcová, L., Anderegg, L.D.L., Hacke, U.G., Berry, J.A., Field, C.B., 2013. Drought's legacy: multiyear hydraulic deterioration underlies widespread aspen forest die-off and portends increased future risk. *Glob. Change Biol.* 19, 1188–1196. <https://doi.org/10.1111/gcb.12100>
- Arend, M., Link, R.M., Patthey, R., Hoch, G., Schuldt, B., Kahmen, A., 2021. Rapid hydraulic collapse as cause of drought-induced mortality in conifers. *Proc. Natl. Acad. Sci.* 118, e2025251118.
<https://doi.org/10.1073/pnas.2025251118>
- Banerjee, O., Bark, R., Connor, J., Crossman, N.D., 2013. An ecosystem services approach to estimating economic losses associated with drought. *Ecol. Econ.* 91, 19–27. <https://doi.org/10.1016/j.ecolecon.2013.03.022>
- Benoit Héloïse. 2022. Evaluating the pertinence of Species Distribution Models for predicting tree vulnerability, using a retrospective approach.
- Bianchi, E., Bugmann, H., Bigler, C., 2021. Light availability predicts mortality probability of conifer saplings in Swiss mountain forests better than radial growth and tree size. *For. Ecol. Manag.* 479, 118607.
<https://doi.org/10.1016/j.foreco.2020.118607>
- Bigler, C., Bugmann, H., 2004. Assessing the performance of theoretical and empirical tree mortality models using tree-ring series of Norway spruce. *Ecol. Model.* 174, 225–239. <https://doi.org/10.1016/j.ecolmodel.2003.09.025>
- Blackman, C.J., Pfautsch, S., Choat, B., Delzon, S., Gleason, S.M., Duursma, R.A., 2016. Toward an index of desiccation time to tree mortality under drought: Desiccation time to tree mortality. *Plant Cell Environ.* 39, 2342–2345.
<https://doi.org/10.1111/pce.12758>
- Brienen, R.J.W., Phillips, O.L., Feldpausch, T.R., Gloor, E., Baker, T.R., Lloyd, J., Lopez-Gonzalez, G., Monteagudo-Mendoza, A., Malhi, Y., Lewis, S.L., Vásquez Martínez, R., Alexiades, M., Álvarez Dávila, E., Alvarez-Loayza, P., Andrade, A., Aragão, L.E.O.C., Araujo-Murakami, A., Arends, E.J.M.M., Arroyo, L., Aymard C., G.A., Bánki, O.S., Baraloto, C., Barroso, J., Bonal, D., Boot, R.G.A., Camargo, J.L.C., Castilho, C.V., Chama, V., Chao, K.J., Chave, J., Comiskey, J.A., Cornejo Valverde, F., Da Costa, L., De Oliveira, E.A., Di Fiore, A., Erwin, T.L., Fauset, S., Forsthofer, M., Galbraith, D.R., Grahame, E.S., Groot, N., Héault, B., Higuchi, N., Honorio Coronado, E.N., Keeling, H., Killeen, T.J., Laurance, W.F., Laurance, S., Licona, J., Magnussen, W.E., Marimon, B.S., Marimon-Junior, B.H., Mendoza, C., Neill, D.A., Nogueira, E.M., Núñez, P., Pallqui Camacho, N.C., Parada, A., Pardo-Molina, G., Peacock, J., Peña-Claros, M., Pickavance, G.C., Pitman, N.C.A., Poorter, L., Prieto, A., Quesada, C.A., Ramírez, F., Ramírez-Angulo, H., Restrepo, Z., Roopsind, A., Rudas, A.,

- Salomão, R.P., Schwarz, M., Silva, N., Silva-Espejo, J.E., Silveira, M., Stropp, J., Talbot, J., Ter Steege, H., Teran-Aguilar, J., Terborgh, J., Thomas-Caesar, R., Toledo, M., Torello-Raventos, M., Umetsu, R.K., Van Der Heijden, G.M.F., Van Der Hout, P., Guimarães Vieira, I.C., Vieira, S.A., Vilanova, E., Vos, V.A., Zagt, R.J., 2015. Long-term decline of the Amazon carbon sink. *Nature* 519, 344–348. <https://doi.org/10.1038/nature14283>
- Brodribb, T.J., 2020. Learning from a century of droughts. *Nat. Ecol. Evol.* 4, 1007–1008. <https://doi.org/10.1038/s41559-020-1226-2>
- Bugmann, H., 2001. A review of forest gap models. *Clim. Change* 51, 259–305. <https://doi.org/10.1023/A:1012525626267>
- Bugmann, H., Seidl, R., Hartig, F., Bohn, F., Brůna, J., Cailleret, M., François, L., Heinke, J., Henrot, A.-J., Hickler, T., Hülsmann, L., Huth, A., Jacquemin, I., Kollas, C., Lasch-Born, P., Lexer, M.J., Merganič, J., Merganičová, K., Mette, T., Miranda, B.R., Nadal-Sala, D., Rammer, W., Rammig, A., Reineking, B., Roedig, E., Sabaté, S., Steinkamp, J., Suckow, F., Vacchiano, G., Wild, J., Xu, C., Reyer, C.P.O., 2019. Tree mortality submodels drive simulated long-term forest dynamics: assessing 15 models from the stand to global scale. *Ecosphere* 10, e02616. <https://doi.org/10.1002/ecs2.2616>
- Cailleret, M., Nourtier, M., Amm, A., Durand-Gillmann, M., Davi, H., 2014. Drought-induced decline and mortality of silver fir differ among three sites in Southern France. *Ann. For. Sci.* 71, 643–657. <https://doi.org/10.1007/s13595-013-0265-0>
- Campbell, G.S., 1986. Soil Physics with Basic. 1986: Soil Sci. 142, 367–368. <https://doi.org/10.1097/00010694-198612000-00007>
- Campbell, G.S., Campbell, G.S., 1977. An Introduction to Environmental Biophysics, Heidelberg Science Library. Springer New York, New York, NY. <https://doi.org/10.1007/978-1-4684-9917-9>
- Caudullo, G., Tinner, W., de Rigo, D., n.d. *Picea abies* in Europe: distribution, habitat, usage and threats.
- Choat, B., Brodribb, T.J., Brodersen, C.R., Duursma, R.A., Lopez, R., Medlyn, B.E., 2018. Triggers of tree mortality under drought. *Nature* 558, 531–539. <https://doi.org/10.1038/s41586-018-0240-x>
- Choat, B., Jansen, S., Brodribb, T.J., Cochard, H., Delzon, S., Bhaskar, R., Bucci, S.J., Feild, T.S., Gleason, S.M., Hacke, U.G., Jacobsen, A.L., Lens, F., Maherali, H., Martínez-Vilalta, J., Mayr, S., Mencuccini, M., Mitchell, P.J., Nardini, A., Pittermann, J., Pratt, R.B., Sperry, J.S., Westoby, M., Wright, I.J., Zanne, A.E., 2012. Global convergence in the vulnerability of forests to drought. *Nature* 491, 752–755. <https://doi.org/10.1038/nature11688>
- Christoffersen, B.O., Gloor, M., Fauset, S., Fyllas, N.M., Galbraith, D.R., Baker, T.R., Kruijt, B., Rowland, L., Fisher, R.A., Binks, O.J., Sevanto, S., Xu, C., Jansen, S., Choat, B., Mencuccini, M., McDowell, N.G., Meir, P., 2016. Linking hydraulic traits to tropical forest function in a size-structured and trait-driven model (TFS v.1-Hydro). *Geosci. Model Dev.* 9, 4227–4255. <https://doi.org/10.5194/gmd-9-4227-2016>
- Chuine, I., Beaubien, E.G., 2001. Phenology is a major determinant of tree species range. *Ecol. Lett.* 4, 500–510. <https://doi.org/10.1046/j.1461-0248.2001.00261.x>
- Cochard, H., Pimont, F., Ruffault, J., Martin-StPaul, N., 2021. SurEau: a mechanistic model of plant water relations under extreme drought. *Ann. For. Sci.* 78, 55. <https://doi.org/10.1007/s13595-021-01067-y>
- Davi, H., Cailleret, M., 2017. Assessing drought-driven mortality trees with physiological process-based models. *Agric. For. Meteorol.* 232, 279–290. <https://doi.org/10.1016/j.agrformet.2016.08.019>
- Dobrowolska, D., Bončina, A., Klumpp, R., 2017. Ecology and silviculture of silver fir (*Abies alba* Mill.): a review. *J. For. Res.* 22, 326–335. <https://doi.org/10.1080/13416979.2017.1386021>
- Druel, A., Martins, N., Cochard, H., DeCaceres, M., Delzon, S., Mencuccini, M., Torres-Ruiz, J., Ruffault, J., 2023. European forest vulnerability to hydraulic failure: an ecohydrological approach (other). display. <https://doi.org/10.5194/egusphere-egu23-17068>

- Eagleson, P.S., 1982. Ecological optimality in water-limited natural soil-vegetation systems: 1. Theory and hypothesis. *Water Resour. Res.* 18, 325–340. <https://doi.org/10.1029/WR018i002p00325>
- Elith, J., H. Graham, C., P. Anderson, R., Dudík, M., Ferrier, S., Guisan, A., J. Hijmans, R., Huettmann, F., R. Leathwick, J., Lehmann, A., Li, J., G. Lohmann, L., A. Loiselle, B., Manion, G., Moritz, C., Nakamura, M., Nakazawa, Y., McC. M. Overton, J., Townsend Peterson, A., J. Phillips, S., Richardson, K., Scachetti-Pereira, R., E. Schapire, R., Soberón, J., Williams, S., S. Wisz, M., E. Zimmermann, N., 2006. Novel methods improve prediction of species' distributions from occurrence data. *Ecography* 29, 129–151. <https://doi.org/10.1111/j.2006.0906-7590.04596.x>
- Fridman, J., Stahl, G., 2001. A three-step approach for modelling tree mortality in Swedish forests. *Scand. J. For. Res.* 16, 455–466. <https://doi.org/10.1080/02827580152632856>
- Gonçalves, A.F.A., Santos, J.A.D., França, L.C.D.J., Campoe, O.C., Altoé, T.F., Scolforo, J.R.S., 2021. Use of the process-based models in forest research: a bibliometric review. *CERNE* 27, e-102769. <https://doi.org/10.1590/01047760202127012769>
- Guisan, A., Zimmermann, N.E., 2000. Predictive habitat distribution models in ecology. *Ecol. Model.* 135, 147–186. [https://doi.org/10.1016/S0304-3800\(00\)00354-9](https://doi.org/10.1016/S0304-3800(00)00354-9)
- Hammond, W.M., Williams, A.P., Abatzoglou, J.T., Adams, H.D., Klein, T., López, R., Sáenz-Romero, C., Hartmann, H., Breshears, D.D., Allen, C.D., 2022. Global field observations of tree die-off reveal hotter-drought fingerprint for Earth's forests. *Nat. Commun.* 13, 1761. <https://doi.org/10.1038/s41467-022-29289-2>
- Harmon, M.E., Bell, D.M., 2020. Mortality in Forested Ecosystems: Suggested Conceptual Advances. *Forests* 11, 572. <https://doi.org/10.3390/f11050572>
- Hasenauer, H., Merkl, D., Weingartner, M., 2001. Estimating tree mortality of Norway spruce stands with neural networks. *Adv. Environ. Res.* 5, 405–414. [https://doi.org/10.1016/S1093-0191\(01\)00092-2](https://doi.org/10.1016/S1093-0191(01)00092-2)
- Huang, J., Kautz, M., Trowbridge, A.M., Hammerbacher, A., Raffa, K.F., Adams, H.D., Goodisman, D.W., Xu, C., Meddens, A.J.H., Kandasamy, D., Gershenson, J., Seidl, R., Hartmann, H., 2020. Tree defence and bark beetles in a drying world: carbon partitioning, functioning and modelling. *New Phytol.* 225, 26–36. <https://doi.org/10.1111/nph.16173>
- Hubau, W., Lewis, S.L., Phillips, O.L., Affum-Baffoe, K., Beeckman, H., Cuni-Sánchez, A., Daniels, A.K., Ewango, C.E.N., Fauset, S., Mukinzi, J.M., Sheil, D., Sonke, B., Sullivan, M.J.P., Sunderland, T.C.H., Taedoumg, H., Thomas, S.C., White, L.J.T., Abernethy, K.A., Adu-Bredu, S., Amani, C.A., Baker, T.R., Banin, L.F., Baya, F., Begne, S.K., Bennett, A.C., Benedet, F., Bitariho, R., Bocko, Y.E., Boeckx, P., Boundja, P., Brienen, R.J.W., Brncic, T., Chezeaux, E., Chuyong, G.B., Clark, C.J., Collins, M., Comiskey, J.A., Coomes, D.A., Dargie, G.C., de Haulleville, T., Kamdem, M.N.D., Doucet, J.-L., Esquivel-Muelbert, A., Feldpausch, T.R., Fofanah, A., Foli, E.G., Gilpin, M., Gloor, E., Gonmadje, C., Gourlet-Fleury, S., Hall, J.S., Hamilton, A.C., Harris, D.J., Hart, T.B., Hockemba, M.B.N., Hladik, A., Ifo, S.A., Jeffery, K.J., Jucker, T., Yakusu, E.K., Kearsley, E., Kenfack, D., Koch, A., Leal, M.E., Levesley, A., Lindsell, J.A., Lisingo, J., Lopez-Gonzalez, G., Lovett, J.C., Makana, J.-R., Malhi, Y., Marshall, A.R., Martin, J., Martin, E.H., Mbayu, F.M., Medjibe, V.P., Mihindou, V., Mitchard, E.T.A., Moore, S., Munishi, P.K.T., Bengone, N.N., Ojo, L., Ondo, F.E., Peh, K.S.-H., Pickavance, G.C., Poulsen, A.D., Poulsen, J.R., Qie, L., Reitsma, J., Rovero, F., Swaine, M.D., Talbot, J., Taplin, J., Taylor, D.M., Thomas, D.W., Toirambe, B., Mukendi, J.T., Tuagben, D., Umunay, P.M., van der Heijden, G.M.F., Verbeeck, H., Vleminckx, J., Willcock, S., Woll, H., Woods, J.T., Zemagho, L., 2020. Asynchronous carbon sink saturation in African and Amazonian tropical forests. *Nature* 579, 80–+. <https://doi.org/10.1038/s41586-020-2035-0>
- Hulsmann, L., Bugmann, H., Cailleret, M., Brang, P., 2018. How to kill a tree: empirical mortality models for 18 species and their performance in a dynamic forest model. *Ecol. Appl.* 28, 522–540. <https://doi.org/10.1002/eap.1668>

- Hülsmann Lisa (2021, May 5th). Tree mortality modeling - a tool for ecological inference and a challenge for projecting forest dynamics [Video]. YouTube. <https://www.youtube.com/watch?v=Yzsa0p7lq7c&t=1s>
- Jourdan Marion, in review. Using climate-sensitive forest models to provide guidance for adaptive forest management under climate change.
- Keane, R.E., Austin, M., Field, C., Huth, A., Lexer, M.J., Peters, D., Solomon, A., Wyckoff, P., 2001. Tree mortality in gap models: Application to climate change. *Clim. Change* 51, 509–540. <https://doi.org/10.1023/A:1012539409854>
- King, S.L., 1996. Logistic regression vs. neural networks for predicting individual-tree mortality. *Proc. 1996 Soc. Am. For. Conv. Diverse For. Abund. Oppor. Evol. Realities* 448–450.
- Krejza, J., Cienciala, E., Světlík, J., Bellan, M., Noyer, E., Horáček, P., Štěpánek, P., Marek, M.V., 2021. Evidence of climate-induced stress of Norway spruce along elevation gradient preceding the current dieback in Central Europe. *Trees* 35, 103–119. <https://doi.org/10.1007/s00468-020-02022-6>
- Lévesque, M., Saurer, M., Siegwolf, R., Eilmann, B., Brang, P., Bugmann, H., Rigling, A., 2013. Drought response of five conifer species under contrasting water availability suggests high vulnerability of Norway spruce and European larch. *Glob. Change Biol.* 19, 3184–3199. <https://doi.org/10.1111/gcb.12268>
- Li, X., Xi, B., Wu, X., Choat, B., Feng, J., Jiang, M., Tissue, D., 2022. Unlocking Drought-Induced Tree Mortality: Physiological Mechanisms to Modeling. *Front. Plant Sci.* 13, 835921. <https://doi.org/10.3389/fpls.2022.835921>
- Liu, Q., Peng, C., Schneider, R., Cyr, D., Liu, Z., Zhou, X., Kneeshaw, D., 2021. TRIPLEX-Mortality model for simulating drought-induced tree mortality in boreal forests: Model development and evaluation. *Ecol. Model.* 455, 109652. <https://doi.org/10.1016/j.ecolmodel.2021.109652>
- Liu, Q., Peng, C., Schneider, R., Cyr, D., McDowell, N.G., Kneeshaw, D., 2023. Drought-induced increase in tree mortality and corresponding decrease in the carbon sink capacity of Canada's boreal forests from 1970 to 2020. *Glob. Change Biol.* 29, 2274–2285. <https://doi.org/10.1111/gcb.16599>
- Manion, P.D., 1991. *Tree Disease Concepts*. Prentice Hall.
- Maringer, J., Stelzer, A.-S., Paul, C., Albrecht, A.T., 2021. Ninety-five years of observed disturbance-based tree mortality modeled with climate-sensitive accelerated failure time models. *Eur. J. For. Res.* 140, 255–272. <https://doi.org/10.1007/s10342-020-01328-x>
- Martinez-Vilalta, J., Anderegg, W.R.L., Sapes, G., Sala, A., 2019. Greater focus on water pools may improve our ability to understand and anticipate drought-induced mortality in plants. *New Phytol.* 223, 22–32. <https://doi.org/10.1111/nph.15644>
- Martínez-Vilalta, J., Piñol, J., Beven, K., 2002. A hydraulic model to predict drought-induced mortality in woody plants: an application to climate change in the Mediterranean. *Ecol. Model.* 155, 127–147. [https://doi.org/10.1016/S0304-3800\(02\)00025-X](https://doi.org/10.1016/S0304-3800(02)00025-X)
- McDowell, N., Pockman, W.T., Allen, C.D., Breshears, D.D., Cobb, N., Kolb, T., Plaut, J., Sperry, J., West, A., Williams, D.G., Yepez, E.A., 2008. Mechanisms of plant survival and mortality during drought: why do some plants survive while others succumb to drought? *New Phytol.* 178, 719–739. <https://doi.org/10.1111/j.1469-8137.2008.02436.x>
- McDowell, N.G., Beerling, D.J., Breshears, D.D., Fisher, R.A., Raffa, K.F., Stitt, M., 2011. The interdependence of mechanisms underlying climate-driven vegetation mortality. *Trends Ecol. Evol.* 26, 523–532. <https://doi.org/10.1016/j.tree.2011.06.003>
- McDowell, N.G., Fisher, R.A., Xu, C., Domec, J.C., Hölttä, T., Mackay, D.S., Sperry, J.S., Boutz, A., Dickman, L., Gehres, N., Limousin, J.M., Macalady, A., Martínez-Vilalta, J., Mencuccini, M., Plaut, J.A., Ogée, J., Pangle, R.E., Rasse, D.P., Ryan, M.G., Sevanto, S., Waring, R.H., Williams, A.P., Yepez, E.A., Pockman, W.T., 2013.

- Evaluating theories of drought-induced vegetation mortality using a multimodel–experiment framework. *New Phytol.* 200, 304–321. <https://doi.org/10.1111/nph.12465>
- McDowell, N.G. (2021, March 24th). Rising tree mortality in the Anthropocene [Video]. YouTube.
<https://www.youtube.com/watch?v=vdAXQ8CibKA&t=1s>
- McDowell, N.G., Sapes, G., Pivovaroff, A., Adams, H.D., Allen, C.D., Anderegg, W.R.L., Arend, M., Breshears, D.D., Brodribb, T., Choat, B., Cochard, H., De Cáceres, M., De Kauwe, M.G., Grossiord, C., Hammond, W.M., Hartmann, H., Hoch, G., Kahmen, A., Klein, T., Mackay, D.S., Mantova, M., Martínez-Vilalta, J., Medlyn, B.E., Mencuccini, M., Nardini, A., Oliveira, R.S., Sala, A., Tissue, D.T., Torres-Ruiz, J.M., Trowbridge, A.M., Trugman, A.T., Wiley, E., Xu, C., 2022. Mechanisms of woody-plant mortality under rising drought, CO₂ and vapour pressure deficit. *Nat. Rev. Earth Environ.* 3, 294–308. <https://doi.org/10.1038/s43017-022-00272-1>
- Meir, P., Mencuccini, M., Dewar, R.C., 2015. Drought-related tree mortality: addressing the gaps in understanding and prediction. *New Phytol.* 207, 28–33. <https://doi.org/10.1111/nph.13382>
- Mensah, C., Šigut, L., Fischer, M., Foltýnová, L., Jocher, G., Acosta, M., Kowalska, N., Kokrda, L., Pavelka, M., Marshall, J.D., Nyantakyi, E.K., Marek, M.V., 2021. Assessing the Contrasting Effects of the Exceptional 2015 Drought on the Carbon Dynamics in Two Norway Spruce Forest Ecosystems. *Atmosphere* 12, 988. <https://doi.org/10.3390/atmos12080988>
- Morin, X., Bugmann, H., Coligny, F., Martin-StPaul, N., Cailleret, M., Limousin, J., Ourcival, J., Prevosto, B., Simioni, G., Toigo, M., Vennetier, M., Catteau, E., Guillemot, J., 2021. Beyond forest succession: A gap model to study ecosystem functioning and tree community composition under climate change. *Funct. Ecol.* 35, 955–975. <https://doi.org/10.1111/1365-2435.13760>
- Muñoz-Sabater, J., Dutra, E., Agustí-Panareda, A., Albergel, C., Arduini, G., Balsamo, G., Boussetta, S., Choulga, M., Harrigan, S., Hersbach, H., Martens, B., Miralles, D.G., Piles, M., Rodríguez-Fernández, N.J., Zsoter, E., Buontempo, C., Thépaut, J.-N., 2021. ERA5-Land: a state-of-the-art global reanalysis dataset for land applications. *Earth Syst. Sci. Data* 13, 4349–4383. <https://doi.org/10.5194/essd-13-4349-2021>
- Panagos, P., Van Liedekerke, M., Jones, A., Montanarella, L., 2012. European Soil Data Centre: Response to European policy support and public data requirements. *Land Use Policy* 29, 329–338. <https://doi.org/10.1016/j.landusepol.2011.07.003>
- Peng, C., Ma, Z., Lei, X., Zhu, Q., Chen, H., Wang, W., Liu, S., Li, W., Fang, X., Zhou, X., 2011. A drought-induced pervasive increase in tree mortality across Canada’s boreal forests. *Nat. Clim. Change* 1, 467–471. <https://doi.org/10.1038/nclimate1293>
- Piedallu, C., Dallery, D., Bresson, C., Legay, M., Gégout, J.-C., Pierrat, R., 2023. Spatial vulnerability assessment of silver fir and Norway spruce dieback driven by climate warming. *Landsc. Ecol.* 38, 341–361. <https://doi.org/10.1007/s10980-022-01570-1>
- Piedallu, C., Gégout, J.-C., Lebourgeois, F., Seynave, I., 2016. Soil aeration, water deficit, nitrogen availability, acidity and temperature all contribute to shaping tree species distribution in temperate forests. *J. Veg. Sci.* 27, 387–399. <https://doi.org/10.1111/jvs.12370>
- Piedallu, C., Gégout, J.-C., Perez, V., Lebourgeois, F., 2013. Soil water balance performs better than climatic water variables in tree species distribution modelling: Soil water balance improves tree species distribution models. *Glob. Ecol. Biogeogr.* 22, 470–482. <https://doi.org/10.1111/geb.12012>
- Postic Tanguy. 2022. Estimating the sensibility and adaptation of French forests to climate-chance through a coupling of process-based models.
- Rohner, B., Bigler, C., Wunder, J., Brang, P., Bugmann, H., 2012. Fifty years of natural succession in Swiss forest reserves: changes in stand structure and mortality rates of oak and beech. *J. Veg. Sci.* 23, 892–905. <https://doi.org/10.1111/j.1654-1103.2012.01408.x>

- Ruffault, J., Pimont, F., Cochard, H., Dupuy, J.-L., Martin-StPaul, N., 2022. SurEau-Ecos v2.0: a trait-based plant hydraulics model for simulations of plant water status and drought-induced mortality at the ecosystem level. *Geosci. Model Dev.* 15, 5593–5626. <https://doi.org/10.5194/gmd-15-5593-2022>
- Ruiz-Benito, P., Vacchiano, G., Lines, E.R., Reyer, C.P.O., Ratcliffe, S., Morin, X., Hartig, F., Mäkelä, A., Yousefpour, R., Chaves, J.E., Palacios-Orueta, A., Benito-Garzón, M., Morales-Molino, C., Camarero, J.J., Jump, A.S., Kattge, J., Lehtonen, A., Ibrom, A., Owen, H.J.F., Zavala, M.A., 2020. Available and missing data to model impact of climate change on European forests. *Ecol. Model.* 416, 108870. <https://doi.org/10.1016/j.ecolmodel.2019.108870>
- Sala, A., Piper, F., Hoch, G., 2010. Physiological mechanisms of drought-induced tree mortality are far from being resolved. *New Phytol.* 186, 274–281. <https://doi.org/10.1111/j.1469-8137.2009.03167.x>
- Seidl, R., Fernandes, P.M., Fonseca, T.F., Gillet, F., Jonsson, A.M., Merganicova, K., Netherer, S., Arpacı, A., Bontemps, J.-D., Bugmann, H., Ramon Gonzalez-Olabarria, J., Lasch, P., Meredieu, C., Moreira, F., Schelhaas, M.-J., Mohren, F., 2011. Modelling natural disturbances in forest ecosystems: a review. *Ecol. Model.* 222, 903–924. <https://doi.org/10.1016/j.ecolmodel.2010.09.040>
- Senf, C., Buras, A., Zang, C.S., Rammig, A., Seidl, R., 2020. Excess forest mortality is consistently linked to drought across Europe. *Nat. Commun.* 11, 6200. <https://doi.org/10.1038/s41467-020-19924-1>
- Sheil, D., 1995. A critique of permanent plot methods and analysis with examples from Budongo Forest, Uganda. *For. Ecol. Manag.* 77, 11–34. [https://doi.org/10.1016/0378-1127\(95\)03583-V](https://doi.org/10.1016/0378-1127(95)03583-V)
- Stewart, G.H., 1986. A theory of forest dynamics. *J. R. Soc. N. Z.* 16, 118–119. <https://doi.org/10.1080/03036758.1986.10426961>
- Suarez, M.L., Ghermandi, L., Kitzberger, T., 2004. Factors predisposing episodic drought-induced tree mortality in Nothofagus—site, climatic sensitivity and growth trends. *J. Ecol.* 92, 954–966. <https://doi.org/10.1111/j.1365-2745.2004.00941.x>
- Taccoen, A., Piedallu, C., Seynave, I., Perez, V., Gégout-Petit, A., Nageleisen, L.-M., Bontemps, J.-D., Gégout, J.-C., 2019. Background mortality drivers of European tree species: climate change matters. *Proc. R. Soc. B Biol. Sci.* 286, 20190386. <https://doi.org/10.1098/rspb.2019.0386>
- Thiele, J.C., Nuske, R.S., Ahrends, B., Panferov, O., Albert, M., Staupendahl, K., Junghans, U., Jansen, M., Saborowski, J., 2017. Climate change impact assessment-A simulation experiment with Norway spruce for a forest district in Central Europe. *Ecol. Model.* 346, 30–47. <https://doi.org/10.1016/j.ecolmodel.2016.11.013>
- Thriplleton, T., Huelsmann, L., Cailleret, M., Bugmann, H., 2021. An evaluation of multi-species empirical tree mortality algorithms for dynamic vegetation modelling. *Sci. Rep.* 11, 19845. <https://doi.org/10.1038/s41598-021-98880-2>
- Trugman, A.T., Anderegg, L.D.L., Anderegg, W.R.L., Das, A.J., Stephenson, N.L., 2021. Why is Tree Drought Mortality so Hard to Predict? *Trends Ecol. Evol.* 36, 520–532. <https://doi.org/10.1016/j.tree.2021.02.001>
- Van Mantgem, P.J., Stephenson, N.L., Byrne, J.C., Daniels, L.D., Franklin, J.F., Fulé, P.Z., Harmon, M.E., Larson, A.J., Smith, J.M., Taylor, A.H., Veblen, T.T., 2009. Widespread Increase of Tree Mortality Rates in the Western United States. *Science* 323, 521–524. <https://doi.org/10.1126/science.1165000>
- Vejpustková, M., Čihák, T., Fišer, P., 2023. The increasing drought sensitivity of silver fir (*Abies alba* Mill.) is evident in the last two decades. *J. For. Sci.* 69, 67–79. <https://doi.org/10.17221/172/2022-JFS>
- Venturas, M.D., Todd, H.N., Trugman, A.T., Anderegg, W.R.L., 2021. Understanding and predicting forest mortality in the western United States using long-term forest inventory data and modeled hydraulic damage. *New Phytol.* 230, 1896–1910. <https://doi.org/10.1111/nph.17043>
- Williamson, G.B., Laurance, W.F., Oliveira, A.A., Delamonica, P., Gascon, C., Lovejoy, T.E., Pohl, L., 2000. Amazonian Tree Mortality during the 1997 El Niño Drought. *Conserv. Biol.* 14, 1538–1542. <https://doi.org/10.1046/j.1523-1739.2000.99298.x>

Appendix

1. Schematic of ForCEEPS and PHENOFIT

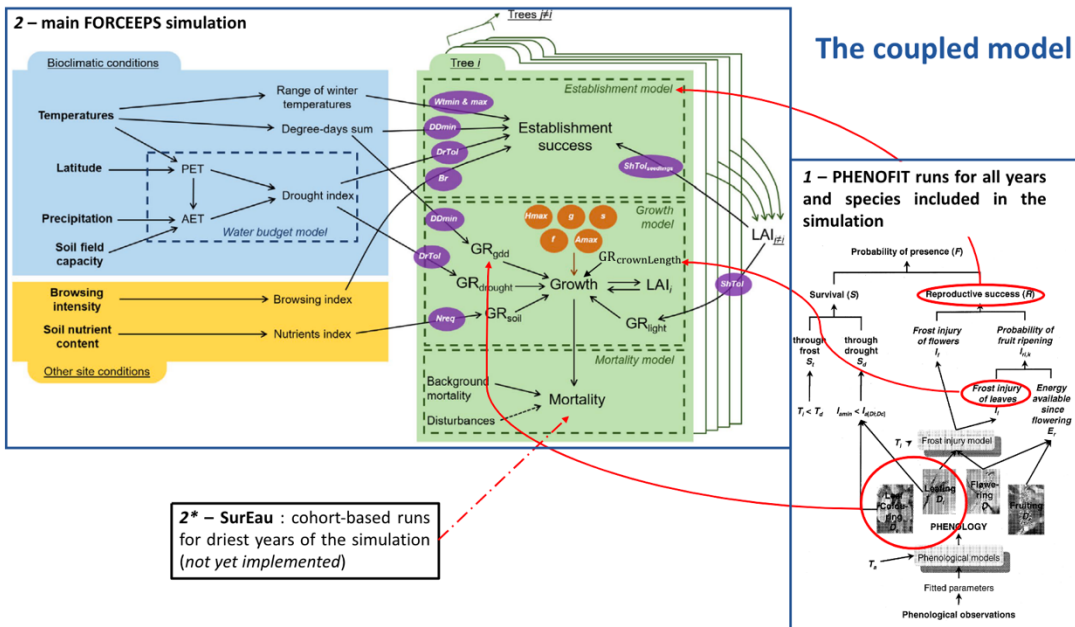


Figure 1. Detailed representation of the processes included in the ForCEEPS and PHENOFIT models. Red circles indicate outputs used for the coupling, and red lines their destination in the ForCEEPS simulation. Original figures are taken from Morin et al. (2021) and Chuine and Beaubien (2001), where parameters details can also be found (Postic, 2022).

2. Species included in NFI dataset

Here in table 1, we listed the species included in NFI dataset and their number of dead trees in total in 1696 plots. And in table 2, it is the species simulated in coupled model and predicted number of dead trees in total in 1696 plots.

Table 1. Species observed in NFI dataset.

Species name	Number of dead trees	Species name	Number of dead trees
<i>Fraxinus excelsior</i>	5416	<i>Ilex aquifolium</i>	58
<i>Picea abies</i>	2961	<i>Arbutus unedo</i>	53
<i>Carpinus betulus</i>	2658	<i>Sorbus torminalis</i>	51
<i>Castanea sativa</i>	2005	<i>Pinus montana</i>	44
<i>Corylus avellana</i>	1235	<i>Acer monspessulanum</i>	42
<i>Abies alba</i>	953	<i>Euonymus europaeus</i>	36
<i>Pinus pinaster</i>	836	<i>Abies grandis</i>	35
<i>Betula pendula</i>	671	<i>Prunus spinosa</i>	34
<i>Populus tremula</i>	641	<i>Pyrus communis</i>	34
<i>Salix caprea</i>	633	<i>Quercus suber</i>	32
<i>Pinus sylvestris</i>	547	<i>Populus x canescens</i>	31

<i>Robinia pseudoacacia</i>	478	<i>Populus nigra</i>	29
<i>Pinus nigra</i>	383	<i>Acer opalus</i>	25
<i>Ulmus minor</i>	316	<i>Prunus domestica</i>	24
<i>Crataegus monogyna</i>	305	<i>Ailanthus altissima</i>	22
<i>Alnus glutinosa</i>	260	<i>Juglans regia</i>	21
<i>Pseudotsuga menziesii</i>	252	<i>Salix atrocinerea</i>	21
<i>Populus</i>	227	<i>Alnus incana</i>	18
<i>Acer pseudoplatanus</i>	205	<i>Juniperus communis</i>	18
<i>Sorbus aria</i>	196	<i>Acer platanoides</i>	17
<i>Sorbus aucuparia</i>	185	<i>Larix kaempferi</i>	17
<i>Prunus avium</i>	173	<i>Populus alba</i>	15
<i>Acer campestre</i>	166	<i>Larix decidua</i>	13
<i>Picea sitchensis</i>	162	<i>Rhus typhina</i>	11
<i>Sambucus nigra</i>	128	<i>Fraxinus angustifolia</i>	9
<i>Tilia platyphyllos</i>	124	<i>Tilia cordata</i>	8
<i>Salix cinerea</i>	120	<i>Rhamnus cathartica</i>	7
<i>Buxus sempervirens</i>	103	<i>Pinus halepensis</i>	5
<i>Salix alba</i>	103	<i>Frangula alnus</i>	3
<i>Malus sylvestris</i>	92	<i>Pinus strobus</i>	3
<i>Laburnum anagyroides</i>	83	<i>Aesculus hippocastanum</i>	1
<i>Ulmus glabra</i>	77	<i>Betula pubescens</i>	1
<i>Prunus mahaleb</i>	66		

Table 2. Species simulated in coupled model.

Species name	Number of dead trees	Species name	Number of dead trees
<i>Angio_Deciduous species*</i>	3808	<i>Tilia cordata</i>	120
<i>Carpinus betulus</i>	2494	<i>Larix decidua</i>	42
<i>Castanea sativa</i>	2032	<i>Pinus montana</i>	41
<i>Fagus sylvatica</i>	1562	<i>Quercus petraea</i>	35
<i>Fraxinus excelsior</i>	881	<i>Alnus incana</i>	32
<i>Tilia platyphyllos</i>	664	<i>Pseudotsuga menziesii</i>	32
<i>Quercus pubescens</i>	654	<i>Populus nigra</i>	26
<i>Acer campestre</i>	569	<i>Quercus ilex</i>	17
<i>Pinus nigra</i>	552	<i>Quercus robur</i>	15
<i>Acer pseudoplatanus</i>	532	<i>Ulmus glabra</i>	12
<i>Gymno_Evergreen species*</i>	434	<i>Sorbus aria</i>	7
<i>Pinus sylvestris</i>	355	<i>Pinus halepensis</i>	4
<i>Corylus avellana</i>	352	<i>Taxus baccata</i>	4
<i>Populus tremula</i>	340	<i>Pinus cembra</i>	3
<i>Betula pendula</i>	314	<i>Sorbus aucuparia</i>	3
<i>Picea abies</i>	272	<i>Angio_Evergreen species*</i>	2
<i>Pinus pinaster</i>	179	<i>Salix alba</i>	2
<i>Abies alba</i>	129		

*They are the standard parameter sets for species which have not been integrated in ForCEEPS.

3. Ecological ingredients covered by Vosges dataset

Regarding the ecological ingredients covered by Vosges dataset, we plotted the average annual rainfall (from 620.70 mm to 1875.70 mm) against average annual temperature (from 6.81 °C to 11.34 °C) as shown below.

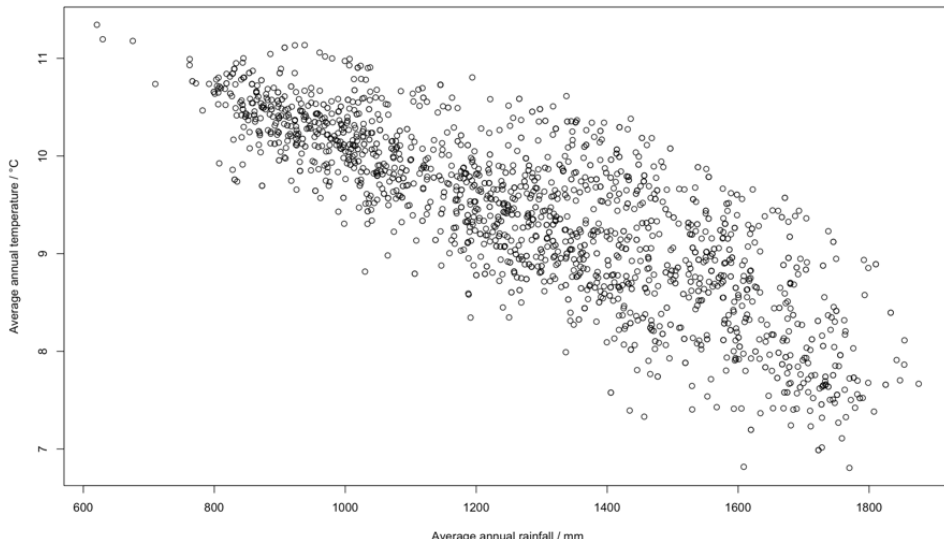


Figure 2. Average annual rainfall against average annual temperature for the 1866 plots from Vosges dataset for Spruce and Fir

4. An example of output files

There are two types of output files: complete file and mean file with .txt format.

Figure 3. Example of complete file.

State	Year	Net/Freeze	Total/Non/soil	Total/Available/Resin	Total/Height/m/ln/ha	Total/Volume/m3/ln/ha	A/L	Drought/ln/Annual	Drought/ln/Des/Annual	Water/ln/Mm(deg)	GDD/annual/(deg day)	GDD/annual/(deg day)	ln/Year	Mean/ln/Resid/Biomass	Biomass/ln/soil	Baseline/ln/soil	Max/ln/soil	Height/m	Height/m	VOLUME/ln/m3	Julian	Feb/Jun	Mar/Jun	Spr/Jun	May/Jun	Julian	Julian	Aug/Sep	
2010	600	308.5682	38.8115	1562.2988	384.1401	13.2282	0.4	0.31288	0.42499	0.4	2181.1592	1411.5626	60	0	31.85682	0	3.8512	1566.22987	39.44061	0	7.05	7.62	7.81	4.42	14.68	10.8	6.47	9.51	3.34
2011	600	311.1165	39.1186	1562.2988	389.0514	13.2282	0.4	0.31288	0.42499	0.4	2181.1592	1411.5626	60	0	31.13865	0	3.9186	1566.4347	39.90156	0	2.11	4.38	5.08	1.38	6.58	5.23	3.95	10.91	3.34
2012	600	313.7644	39.4166	1562.2988	392.0943	13.2282	0.4	0.31288	0.42499	0.4	2181.1592	1411.5626	60	0	31.42048	0	3.9816	1566.6447	40.37241	0	2.11	4.38	5.08	1.38	6.58	5.23	3.95	10.91	3.34
2013	600	314.9779	39.4134	1571.4712	404.4093	11.1393	0.4	0.31276	0.42499	0.4	1895.1592	1766.56772	60	0	31.49729	0	3.96139	1571.2473	40.40493	0	12.26	9.96	9.77	11.33	9.66	6.39	9.51	9.53	9.53
2014	600	310.01511	40.22771	1574.4701	412.9699	13.3015	0.4	0.30448	0.421298	0.4	202.3622	1807.31743	60	0	32.06151	0	4.0277	1574.47021	41.26969	0	10.2	12.25	9.6	9.51	5.51	6.87	5.78	10.45	3.34
2015	580	319.6646	40.86517	1584.4701	411.3044	13.1938	0.4	0.31703	0.32431	0.4	239.4474	1932.7682	58	0	31.90651	0	4.00617	1594.04701	41.43304	0	8.92	7.98	8.99	6.45	4.37	5.43	1.23	11.45	3.34

Figure 4. Example of mean file

5. Explanation of confusion matrix

Table 3. Confusion matrix.

Observation		Mortality plot	Healthy plot
Prediction			
Mortality plot		True positive (TP)	False positive (FP)
Healthy plot		False negative (FN)	True negative (TN)

$$\text{Success of model (SOM)} = \frac{TP+TN}{TP+FP+FN+TN} \quad (\text{Eq. 2})$$

$$\text{Sensitivity (Sn)} = \frac{TP}{TP+FN} \quad (\text{Eq. 3})$$

$$\text{Specificity (Sp)} = \frac{TN}{TN+FP} \quad (\text{Eq. 4})$$

6. Process of extracting LAI Sentinel 2 value

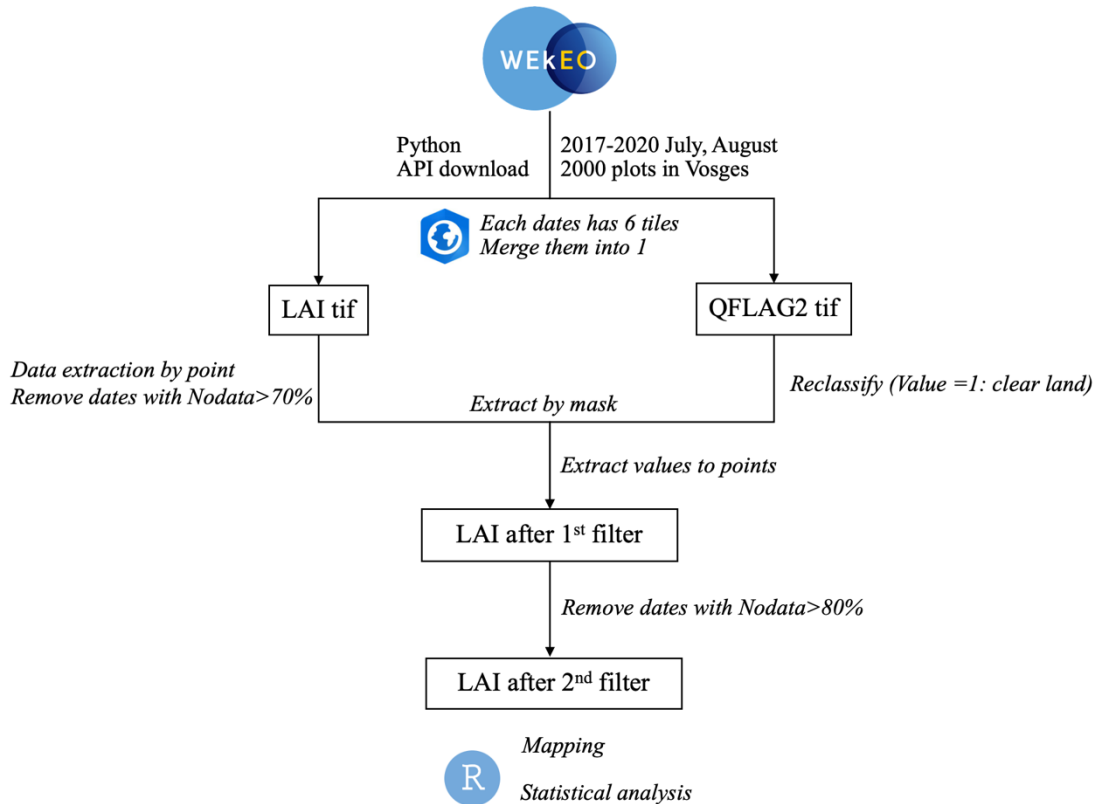


Figure 5. Workflow of LAI preparation from Sentinel 2. LAI: Leaf area index; QFLAG2: Quality Flag data.

7. Confusion matrix for defining plot mortality

Table 4. Confusion matrix of BA loss for Spruce of Vosges dataset.

Prediction \ Observation	Mortality plot	Healthy plot
Prediction		
Mortality plot	335	235
Healthy plot	391	359

Table 5. Confusion matrix of BA loss for Fir of Vosges dataset.

Prediction \ Observation	Mortality plot	Healthy plot
Prediction		
Mortality plot	75	92
Healthy plot	455	576

Table 6. Confusion matrix of BA loss of NFI dataset.

Prediction \ Observation	Mortality plot	Healthy plot
Prediction		
Mortality plot	429	446
Healthy plot	273	546

8. Confusion matrix for comparing soil input data

Table 7. Confusion matrix for Vosges for Modified soil input data.

Prediction \ Observation	Spruce Mortality plot	Spruce Healthy plot	Fir Mortality plot	Fir Healthy plot
Prediction				
Mortality plot	335	235	75	92
Healthy plot	391	359	455	576

Table 8. Confusion matrix for Vosges for Original soil input data.

Prediction \ Observation	Spruce Mortality plot	Spruce Healthy plot	Fir Mortality plot	Fir Healthy plot
Prediction				
Mortality plot	83	49	52	66
Healthy plot	647	458	476	502

Table 9. Confusion matrix for NFI for Modified soil input data.

Prediction \ Observation	Mortality plot	Healthy plot
Prediction		
Mortality plot	429	446
Healthy plot	273	546

Table 10. Confusion matrix for NFI for Original soil input data.

Prediction \ Observation	Mortality plot	Healthy plot
Prediction		
Mortality plot	600	727
Healthy plot	102	266